Supplementary Information

Experimental procedure

DNA binding study

All the experiments involving the binding of the complexes with CT DNA were carried out in deionised water with tris(hydroxymethyl)-aminomethane (Tris, 5 mM) and sodium chloride (50 mM) and adjusted to pH 7.2 with hydrochloric acid at room temperature. The concentration of CT-DNA was determined by UV absorbance at 260 nm. Solutions of CT-DNA in Tris-HCl buffer gave a ratio of UV absorbance at 260 and 280 nm, A_{260}/ A_{280}, of approximately 1.9, indicating that the DNA was sufficiently free of protein. The molar absorption coefficient, ε_{260}, was taken as 6600 M^{-1} cm^{-1}.Various concentrations of CT-DNA (2 - 2.5 μM) was added to the complexes (25 μM dissolved in a DMSO/Tris HCl buffer, 1 % DMSO in the final solution). While measuring the absorption spectra, an equal amount of DNA was added to both the test and reference solutions to eliminate the absorbance of DNA itself. Control experiments with DMSO were performed and no changes in the spectra of CT-DNA were observed. Absorption spectra were recorded after equilibrium at 20° C for 10 min. The intrinsic binding constant K_b was determined by using following equation(1)

$$[DNA]/[\varepsilon_a-\varepsilon_f]) = [DNA]/[\varepsilon_b-\varepsilon_f]+1/K_b[\varepsilon_b-\varepsilon_f] \qquad (S1)$$

The absorption coefficients ε_a , ε_f and ε_b correspond to A_{obsd} / [DNA], the extinction coefficient for the free compound and the extinction coefficient for the compound in the fully bound form respectively. The slope and the intercept of the linear fit of the plot of $[DNA]/[\varepsilon_a -\varepsilon_f]$ versus [DNA] give $1/[\varepsilon_a -\varepsilon_f]$ and $1/K_b[\varepsilon_b-\varepsilon_f]$, respectively. The intrinsic binding constant K_b can be obtained from the ratio of the slope to the intercept. In order to find out the mode of attachment of CT DNA to the compounds fluorescence quenching experiments of EB-DNA were carried out by adding our complexes to the Tris-HCl buffer of EB-DNA. The change in the fluorescence intensity was recorded. Before measurements, the system was shaken well and incubated at room temperature for 5 min. The emission was recorded at 530–750 nm.

Viscosity studies

Viscosity experiments were carried out using a semi-microviscometer maintained at 27 °C in a thermostatic water bath. The DNA concentration was maintained at 100μM, while the compound concentration was varied from 0 to 100 μM. For each sample, the flow time was

measured as triplicate and the average flow time was calculated. The values of relative specific viscosity $(\eta/\eta_0)^{1/3}$ were plotted against 1/R (1/R = [compound]/[DNA]), where η is the relative viscosity of DNA in the presence of the complex and η_0 is the relative viscosity of DNA alone. The relative viscosity (η_0) values were calculated from the observed flow time of the DNA solution (t) corrected for the flow time of the buffer alone (t_0), using the expression $\eta_0 = (t-t_0)/t_0$.

DNA Cleavage Experiment

The cleavage of DNA was monitored using agarose gel electrophoresis. Supercoiled pBR322 DNA (100 ng) in 5 % DMSO and 95 % Tris buffer (5 mM, pH 7.2) with 50 mM NaCl was incubated at 37 °C in the absence and presence of compounds. The DNA, compound and sufficient buffer were premixed in a vial, and the reaction was allowed to proceed for 2 h at 37 °C. The samples were then analyzed by 1.5 % agarose gel electrophoresis in Tris−acetic acid−ethylenediamine tetraacetic acid buffer. The gel was stained with 0.5 μg cm^{-3} ethidium bromide before migration. After electrophoresis at 50 V for 3 h, the gel was illuminated and the digital images were analyzed by gel documentation system (SYNGEN USA).

Serum albumin binding study

Bovine Serum Albumin (BSA) and human serum albumin were purchased from Hi Media, The protein binding study was performed by tryptophan fluorescence quenching experiments using bovine serum albumin (BSA, 10 μM) or human serum albumin (HSA, 10 μM) as the substrate in phosphate buffer (pH= 7.2). Quenching of the emission intensity of tryptophan residues of BSA at 346 nm (excitation wavelength at 280 nm)/ HSA at 345 nm (excitation wavelength at 290 nm) was monitored using ligands and complexes as quenchers with increasing concentration (10-100μM). Synchronous fluorescence spectra of BSA or HSA with various concentrations of the complexes were obtained from 300 to 400 nm when $\Delta\lambda$ = 60 nm and from 290 to 500 nm when $\Delta\lambda$ = 15 nm. For synchronous fluorescence spectra, the same concentrations of serum albumins and the compounds were also used and the spectra were measured at two different $\Delta\lambda$ values (difference between the excitation and emission wavelengths of BSA), such as 15 and 60 nm. Fluorescence and synchronous measurements were performed using a 1 cm quartz cell on a JASCO FP 6600 spectrofluorimeter.

The quenching data can be analyzed according to the Stern-Volmer equation,

$$I_o/I_{corr} = K_{SV}[Q]+1 \qquad \text{Eq (S2)}$$

where I_o is the emission intensity in the absence of compound, I_{corr} is the corrected emission intensity in the presence of compound, K_{SV} is the quenching constant and [Q] is the concentration of the compound.

In order to correct the inner filter effect, the following equation used

$$Icorr = Iobs*10^{(Aexc+Aem)/2}$$

where I_{corr} is the corrected fluorescence value, I_{obs} the measured fluorescence value, A_{exc} is the absorption value at the excitation wavelength, and A_{em} the absorption value at the emission wavelength.

The equilibrium binding constant and the number of binding sites can be analyzed by using Scatchard equation

$$\log [(F_o\text{-}F)/F] = \log K_b + n \log [Q] \qquad \text{Eq (S3)}$$

where, F_o and F are the corrected emission intensities of serum albumins in the absence and presence of the compounds, where n is the binding site per albumin and K_b is the binding constant.

Table S1. Analytical and IR data of the ligands and new Ru(II) complexes

Compound	Elemental analyses Calc. (Found) %				IR spectral data (cm^{-1})					
	C	H	N	S	$\nu_{(C=O\ lactone)}$	$\nu_{C=N}$	$\nu_{(-NH)}$	$\nu_{C=S}$	ν_{C-S}	$\nu_{C\equiv O}$
[H_2-3AC-tsc] (H_2L^1)	55.15 (55.11)	4.25 (4.23)	16.08 (16.04)	12.26 (12.23)	1718	1606	3154	761	-	-
[H_2-3AC-mtsc](H_2L^2)	56.70 (56.67)	4.76 (4.73)	15.26 (15.22)	11.64 (11.62)	1710	1617	3316	762	-	-
[H_2-3AC-etsc] (H_2L^3)	58.10 (58.07)	5.23 (5.20)	14.52 (14.49)	11.07 (11.05)	1722	1615	3315	761	-	-
[H_2-3AC-ptsc] (H_2L^4)	64.06 (64.02)	4.48 (4.46)	12.45 (12.42)	9.50 (9.48)	1711	1610	3205	770	-	-
[Ru(3AC-tsc)(CO)(PPh_3)$_2$]	64.45 (64.43)	4.31 (4.28)	4.60 (4.56)	3.51 (3.47)	1683	1596	-	-	721	1923
[Ru(3AC-mtsc)(CO)(PPh_3)$_2$]	64.77 (64.73)	4.46 (4.43)	4.53 (4.51)	3.45 (3.42)	1687	1594	-	-	743	1919
[Ru(3AC-etsc)(CO)(PPh_3)$_2$]	65.08 (65.06)	4.61 (4.59)	4.46 (4.43)	3.40 (3.36)	1679	1590	-	-	744	1917
[Ru(3AC-ptsc)(CO)(PPh_3)$_2$]	66.78 (66.76)	4.39 (4.36)	4.24 (4.21)	3.24 (3.22)	1671	1595	-	-	746	1917

Table S2. Crystallographic data of the ligands H_2L^{2-3}

Identification code	[H_2-3AC-mtsc)] (H_2L^2)	[H_2-3AC-etsc)](H_2L^3)
Empirical formula	$C_{13}H_{13}N_3O_2S$	$C_{14}H_{15}N_3O_2S$
Formula weight	275.32	389.35
Temperature	90.0(5) K	90.0(5) K
Wavelength	0.71073 Å	0.71073 Å
Crystal system	Monoclinic	Monoclinic
Space group	$P2_1/c$	C 2/c
Unit cell dimensions		
a	9.2790(5) Å	17.2211(8) Å
b	9.6051(5)Å	8.0419(4) Å
c	14.5588(8) Å	20.7942(10) Å
α	90°	90 °
β	90.782(3)°	106.004(3) °
γ	90°	90 °
Volume	1297.44 $Å^3$	2768.18 $Å^3$
Z	4	8
Density	1.409 Mg/m^3	1.389Mg/m^3
Absorption coefficient,	0.251 mm^{-1}	0.239 mm^{-1}
F(000)	576	1216
Crystal size	0.48 × 0.31 × 0.14 mm	0.40 × 0.27 × 0.21 mm
Crystal shape	Plate	Prism
θ range for data collection	2.195 to 36.422 °	2.8777 to 36.365°
Limiting indices	-15 ≤h≤ 15, -15 ≤k≤ 15, -24 ≤l≤ 24	-28 ≤h≤ 28, -13 ≤k≤ 12, -33 ≤l≤ 34
Independent reflections	45883	19810
Absorption correction	multi-scan	multi-scan
Refinement method	Full-matrix least-squares on F^2	Full-matrix least-squares on F^2
Parameters	180	189
Goodness-of-fit on F^2	1.054	1.045
Final R indices [$I>2\sigma(I)$]	R1 = 0.0365, wR2= 0.1013	R1 = 0.0370, wR2= 0.1055
R indices (all data)	R1 = 0.0427, wR2 = 0.1065	R1 = 0.0472, wR2 = 0.0919

Table S3. Selected bond lengths (Å) and bond angles (°) of the ligands H_2L^{2-3}

BOND LENGTHS	H_2L^2	H_2L^3
S1 C12	1.6793(7)	1.682(8)
O1 C9	1.373(1)	1.370(1)
O1 C1	1.367(1)	1.376(1)
O2 C1	1.214(1)	1.209(1)
N1 C10	1.290(1)	1.294(1)
N1 N2	1.3716(9)	1.3677(8)
N2 C12	1.3606(6)	1.374(2)
N2 H2N	0.86(1)	0.91(1)
N3 C12	1.330(1)	1.329(1)
N3 H3N	0.87(1)	0.83(1)
N3 C13	1.448(1)	1.455(1)
C1 C2	1.464(1)	1.466(1)
C2 C3	1.360(1)	1.360(1)
C2 C10	1.481(1)	1.483(1)
C3 C4	1.430(1)	1.429(1)
C3 H3	0.9499(8)	0.9496(9)
C4 C9	1.394(1)	1.392(1)
C4 C5	1.406(1)	1.406(1)
C5 C6	1.384(1)	1.383(1)
C5 H5	0.9504(9)	0.951(1)
C6 C7	1.397(2)	1.396(2)
C6 H6	0.9497(9)	0.949(1)
C7 C8	1.387(1)	1.385(1)
C7 H7	0.950(1)	0.9503(8)
C8 C9	1.391(1)	1.392(1)
BOND ANGLES		
C9 O1 C1	122.72(6)	122.37(7)
C10 N1 N2	118.27(6)	119.07(7)
C12 N2 N1	118.28(6)	117.36(6)
C12 N2 H2N	118.7(9)	117.8(9)
N1 N2 H2N	123.0(9)	124.0(9)
O2 C1 O1	116.36(7)	116.25(8)
O2 C1 C2	126.05(8)	126.63(8)
O1 C1 C2	117.59(7)	117.11(7)
C3 C2 C1	119.24(7)	119.16(7)
C3 C2 C10	121.22(7)	121.17(7)
C1 C2 C10	119.53(6)	119.61(7)
C2 C3 C4	121.40(7)	121.76(8)
C9 C4 C5	118.60(7)	118.62(8)
C9 C4 C3	118.04(7)	117.72(7)
C5 C4 C3	123.24(7)	123.66(8)
C6 C5 C4	120.07(8)	120.08(9)
C5 C6 C7	119.80(9)	119.79(9)
C8 C7 C6	121.41(9)	121.42(9)
C7 C8 C9	117.94(8)	118.02(8)
O1 C9 C4	120.56(7)	120.86(7)
O1 C9 C8	117.27(7)	117.07(7)
C4 C9 C8	122.16(7)	122.07(7)
N1 C10 C2	114.75(6)	113.66(7)
N1 C10 C11	123.65(7)	124.16(7)
C2 C10 C11	121.37(7)	122.12(7)

N3 C12 N2	115.76(6)	116.40(7)
N3 C12 S1	124.33(6)	123.83(6)
N2 C12 S1	119.92(5)	119.78(6)

Table S4. Hydrogen bonds for ligand $\mathbf{H_2L^2}$ [Å and °]

D–H···A	d(D–H)	d(H···A)	d(D···A)	<(DHA)
[H_2-3AC-mtsc]				
N3(A)-H3(A)…O1(B)	0.871	2.698	3.006	61.28
N3(B)-H3(B)…O1(A)	0.871	2.698	3.006	61.28
Symmetry operation: **(x, y, z);** : **(-x, ½+y,1/2-z); (-x, -y, -z); (x, ½-y,1/2+z)**				

Table S5. Antibacterial results of Schiff base ligands $\mathbf{H_2L^{1-4}}$, [RuHClCO(PPh_3)$_3$]and Ru(II) complexes (**1-4**).

Compounds	Concentration (µg/ml)	Zone of inhibition (mm) against bacteria			
		S. aureus	*S. pneumonie*	*P. aeruginosa*	*S. paratyphi*
$\mathbf{H_2L^1}$	25	-	-	-	-
	50	15.19±0.08	15.67±0.43	14.48±0.53	15.55±0.40
	100	17.10±0.22	17.76±0.54	17.44±0.54	18.29±0.11
$\mathbf{H_2L^2}$	25	-	-	-	12.26±0.23
	50	15.22±0.54	15.54±0.33	15.59±0.42	15.34±0.22
	100	17.88±0.11	18.09±0.19	18.22±0.56	18.02±0.65
$\mathbf{H_2L^3}$	25	11.19±0.92	11.19±0.32	-	12.34±0.12
	50	14.02±0.52	14.43±0.65	14.58±0.65	16.66±0.44
		17.82±0.92	17.79±0.12	17.38±0.66	18.10±0.22
$\mathbf{H_2L^4}$	25	-	-	-	-
	50	15.22±0.54	14.29±0.42	15.62±0.22	14.39±0.20
	100	17.88±0.11	17.03±0.14	17.21±0.76	17.44±0.54
Complex **1**	25	-	-	13.20±0.56	-
	50	15.44±0.22	16.88±0.11	14.89±0.11	14.20±0.45
	100	16.76±0.33	18.45±0.33	17.11±0.44	17.10±0.22
Complex **2**	25	12.22±0.56	-	12.89±0.43	11.33±0.56
	50	14.98±0.54	15.02±0.33	14.33±0.43	13.38±0.53
	100	16.65±0.53	18.22±0.52	17.59±0.21	17.02±0.25
Complex **3**	25	13.29±0.64	12.67±0.65	11.87±0.65	12.29±0.32
	50	15.60±0.10	14.48±0.53	13.98±0.55	14.09±0.66
		17.77±0.52	18.09±0.42	17.33±0.24	17.79±0.26
Complex **4**	25	-	-	-	-
	50	14.73±0.34	15.55±0.32	14.09±0.33	14.32±0.22
	100	16.66±0.56	17.83±0.43	17.48±0.45	17.77±0.22
Metal precursor	25	-	-	-	-

	50	15.19±0.08	14.39±0.34	15.78±0.44	13.29±0.65
	100	17.67±0.78	16.44±0.11	17.89±0.42	17.44±0.55
Gentamicin	25	20.32±0.43	20.32±0.39	20.22±0.22	20.39±0.44

Table S6. Antifungal results of Schiff base ligands $\mathbf{H_2L^{1\text{-}4}}$, [$RuHClCO(PPh_3)_3$]and Ru(II) complexes (**1-4**).

Compounds	Concentration (µg/ml)	Zone of inhibition (mm) against fungus				
		C. albicans	*Trichophyton rubrum*	*Aspergillus niger*	*Aspergillus fumigatus*	*Candida tropicalis*
$\mathbf{H_2L^1}$	25	-	11.22±0.11	-	12.89±0.43	-
	50	14.89±0.22	15.23±0.42	15.58±0.61	16.09±0.83	15.38±0.63
	100	17.89±0.45	18.28±0.21	17.15±0.23	19.48±0.45	18.88±0.64
$\mathbf{H_2L^2}$	25	-	-	-	11.01±0.46	-
	50	15.89±0.34	13.31±0.21	14.24±0.63	15.82±0.34	16.32±0.24
	100	17.89±0.66	17.64±0.16	17.91±0.96	18.45±0.44	19.61±0.76
$\mathbf{H_2L^3}$	25	12.54±0.56	-	-	-	-
	50	14.48±0.11	15.34±0.52	13.92±0.43	13.59±0.32	15.28±0.55
		17.77±0.65	17.32±0.13	16.03±0.14	18.22±0.54	18.94±0.52
$\mathbf{H_2L^4}$	25	-	-	10.91±0.12	13.87±0.65	-
	50	14.49±0.54	13.43±0.22	13.25±0.32	15.82±0.72	16.39±0.12
	100	17.29±0.34	16.72±0.86	17.36±0.13	19.21±0.79	18.61±0.42
Complex **1**	25	11.49±0.65	-	11.71±0.65	-	12.87±0.65
	50	13.39±0.22	15.03±0.36	13.48±0.53	16.93±0.83	16.29±0.45
	100	17.89±0.42	17.03±0.64	17.19±0.52	19.59±0.26	19.62±0.53
Complex **2**	25	11.59±0.22	-	-	-	13.89±0.43
	50	14.44±0.54	11.18±0.54	14.01±0.53	16.99±0.81	16.13±0.44
	100	18.02±0.11	17.25±0.13	17.12±0.26	19.11±0.47	19.59±0.23
Complex **3**	25	12.22±0.65	8.24±0.14	-	-	-
	50	13.33±0.11	15.60±0.10	13.32±0.54	16.98±0.85	15.18±0.53
		17.38±0.30	18.17±0.52	16.92±0.25	18.33±0.26	19.33±0.23
Complex **4**	25	-	-	-	-	12.20±0.56
	50	12.29±0.23	14.22±0.21	14.74±0.33	14.18±0.54	16.09±0.36
	100	17.09±0.66	17.56±0.12	16.46±0.14	17.91±0.24	18.48±0.44
Metal precursor	25	-	-	-	-	-
	50	13.29±0.45	14.18±0.54	13.19±0.34	15.58±0.65	14.78±0.43
	100	16.67±0.11	17.91±0.24	15.14±0.31	18.38±0.65	18.59±0.41
Ketaconazole	25	20.34±0.20	24.12±0.16	21.89±0.11	23.01±0.25	19.48±0.23

Table S7. Minimum inhibitory concentration (MIC) in (μM) of the antibacterial studies

COMPOUNDS	IC_{50} VALUES (μM)			
	S. aureus	*S. pneumonie*	*P. aeruginosa*	*S. paratyphi*
Gentamicin	10.00±0.03	7.01±0.09	6.27±0.06	7.00±0.08
H_2L^1	122.03±2.61	112.56±2.40	122.06±2.53	84.03±1.61
H_2L^2	58.83±1.23	100.1±1.73	110.79±2.11	55.47±1.03
H_2L^3	42.00±0.94	56.68±1.33	107.84±1.83	54.14±1.00
H_2L^4	109.58±2.09	91.43±1.44	91.1±1.23	97.07±1.48
$[RuHClCO(PPh_3)_3]$	35.84±0.37	33.05±0.28	30.19±0.53	27.85±0.38
Complex **1**	31.98±0.44	28.74±0.18	18.83±0.22	29.88±0.58
Complex **2**	15.87±0.28	20.83±0.37	17.92±0.19	18.70±0.21
Complex **3**	14.62±0.24	19.00±0.29	16.92±0.32	16.10±0.12
Complex **4**	33.93±0.52	30.79±0.87	27.55±0.32	25.62±0.48

Table S8. Minimum inhibitory concentration (MIC) in (μM) of the antifungal studies

COMPOUNDS	IC_{50} VALUES (μM)				
	Trichophyton rubrum	*Aspergillus niger*	*Aspergillus fumigatus*	*Candida tropicalis*	*C. albicans*
Ketaconazole	10.03±0.09	9.05±0.08	7.56±0.08	7.70±0.10	7.30±0.09
H_2L^1	117.00±2.82	93.75±1.94	92.80±2.13	89.09±1.54	93.06±1.92
H_2L^2	108.13±1.21	88.57±1.54	80.80±1.99	84.79±1.13	87.13±1.53
H_2L^3	85.08±0.87	97.88±1.43	70.75±1.78	45.42±1.11	56.54±1.23
H_2L^4	98.63±2.23	86.99±1.36	85.10±1.58	72.60±1.44	74.97±1.12
$[RuHClCO(PPh_3)_3]$	31.76±0.42	31.63±0.59	29.75±0.54	28.79±0.41	26.09±0.48
Complex **1**	16.87±0.52	15.63±0.18	16.05±0.19	15.64±0.38	15.64±0.21
Complex **2**	15.42±0.23	14.51±0.13	15.24±0.15	14.40±0.29	15.27±0.15
Complex **3**	14.18±0.19	14.29±0.20	13.91±0.20	15.18±0.11	13.86±0.27
Complex **4**	15.84±0.24	24.42±0.37	20.69±0.25	24.58±0.37	22.43±0.44

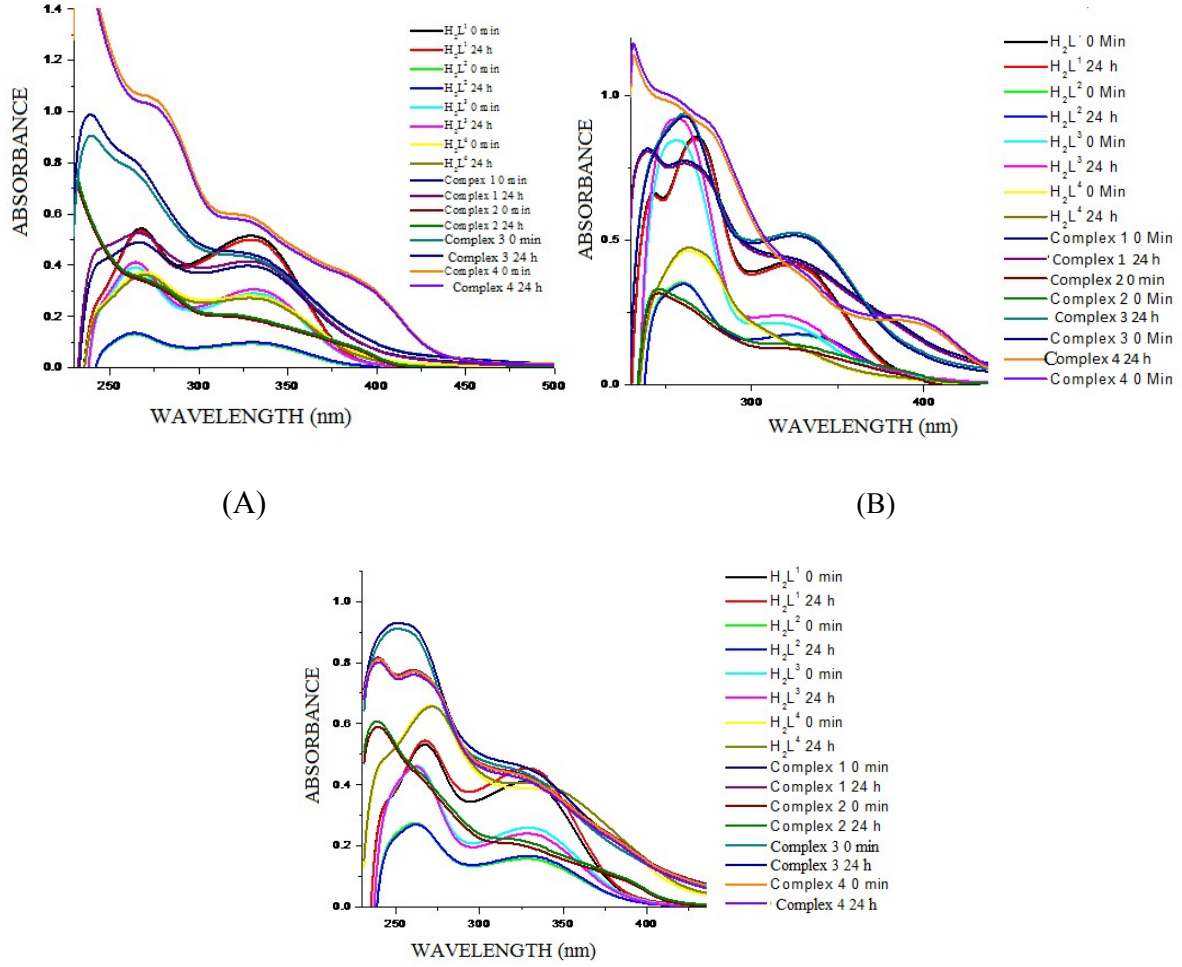

Fig. S1 Stability studies of the complexes using UV-Vis absorption spectroscopic technique. A) absorption spectra of the compounds in 1% aqueous DMSO; B) absorption spectra of the compounds in 99: 1 tris HCl buffer : DMSO C) absorption spectra of the compounds in 99: 1 phosphate buffer: DMSO

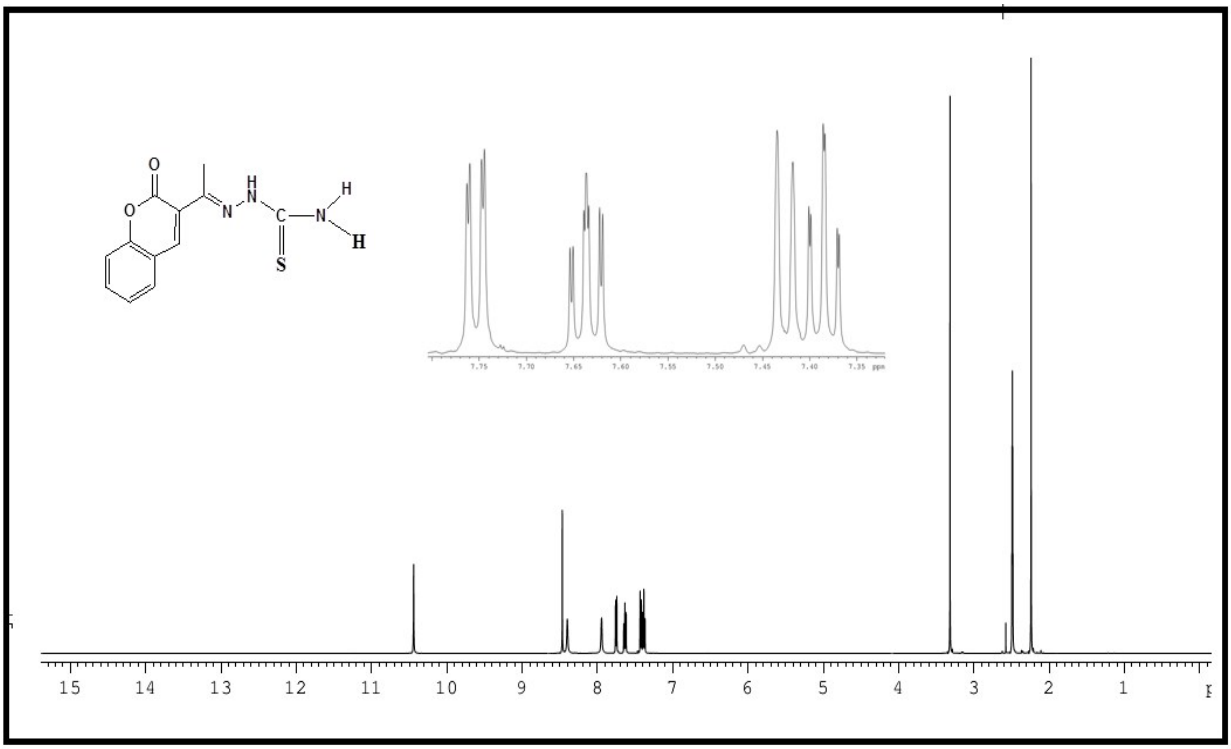

Fig. S2 ^{1}H-NMR spectrum of **[H_2-3AC-tsc] (H_2L^1)**

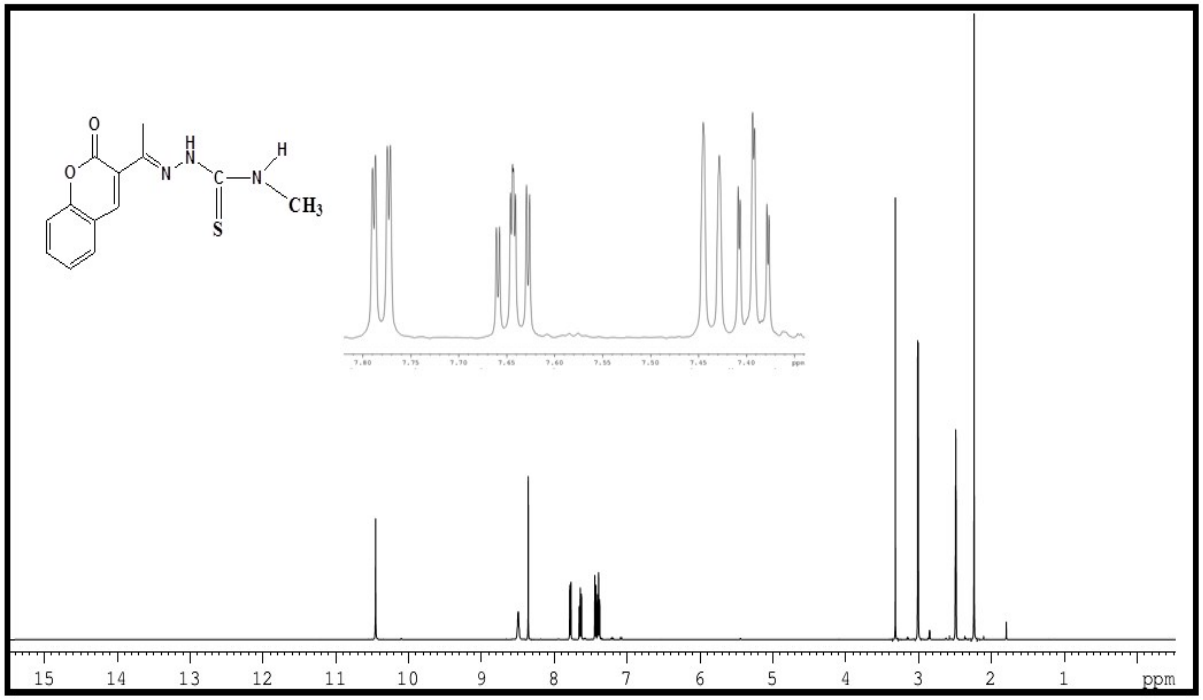

Fig. S3 ^{1}H-NMR spectrum of **[H_2-3AC-mtsc] (H_2L^2)**

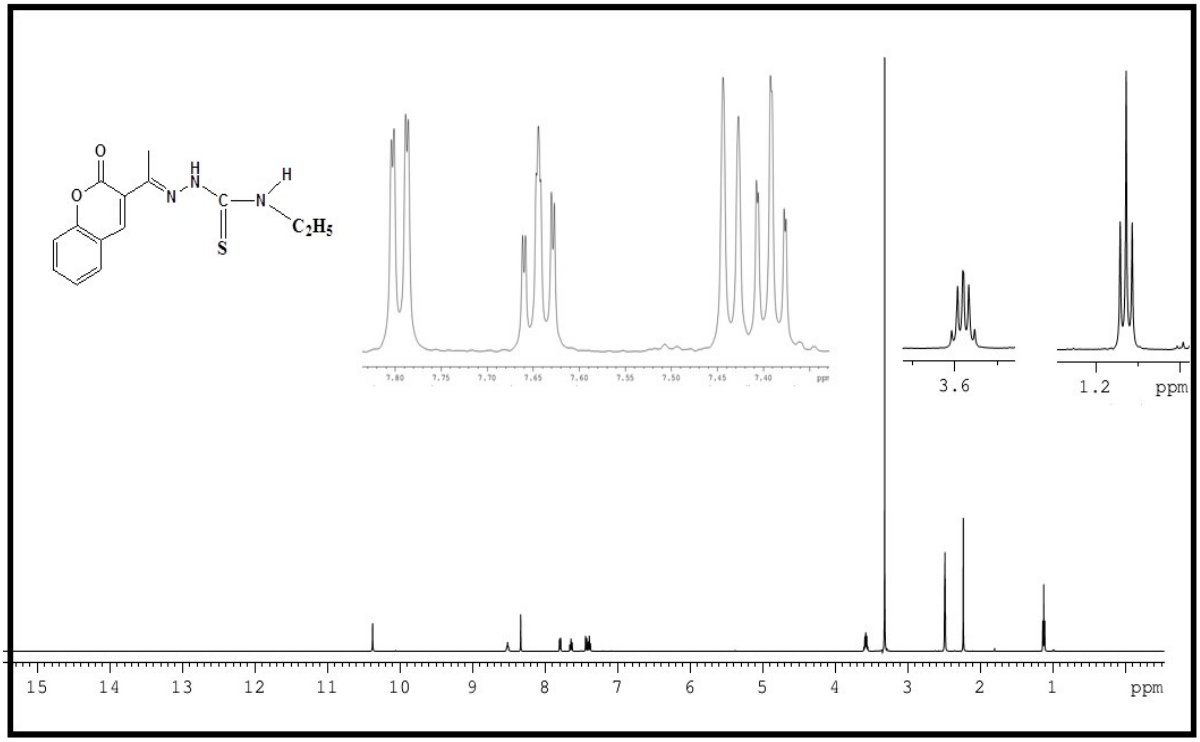

Fig. S4 ^{1}H-NMR spectrum of **[H_2-3AC-etsc] (H_2L^3)**

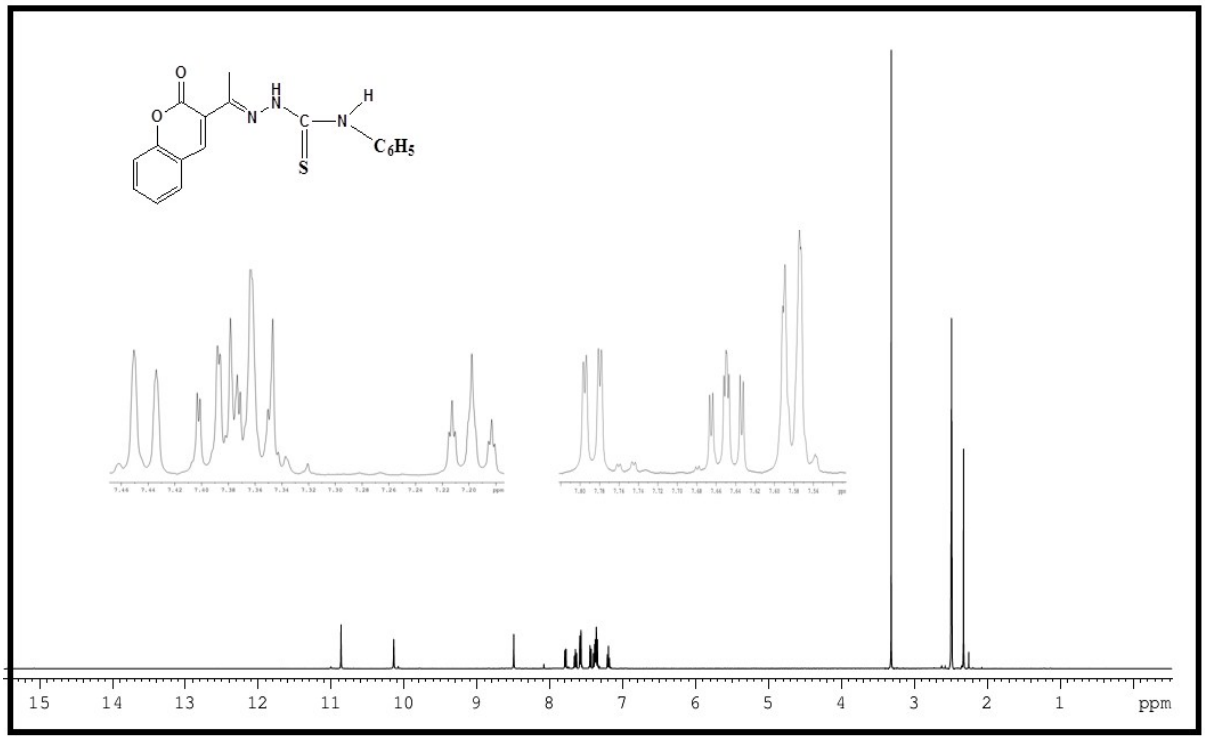

Fig. S5 ^{1}H-NMR spectrum of **[H_2-3AC-ptsc] (H_2L^4)**

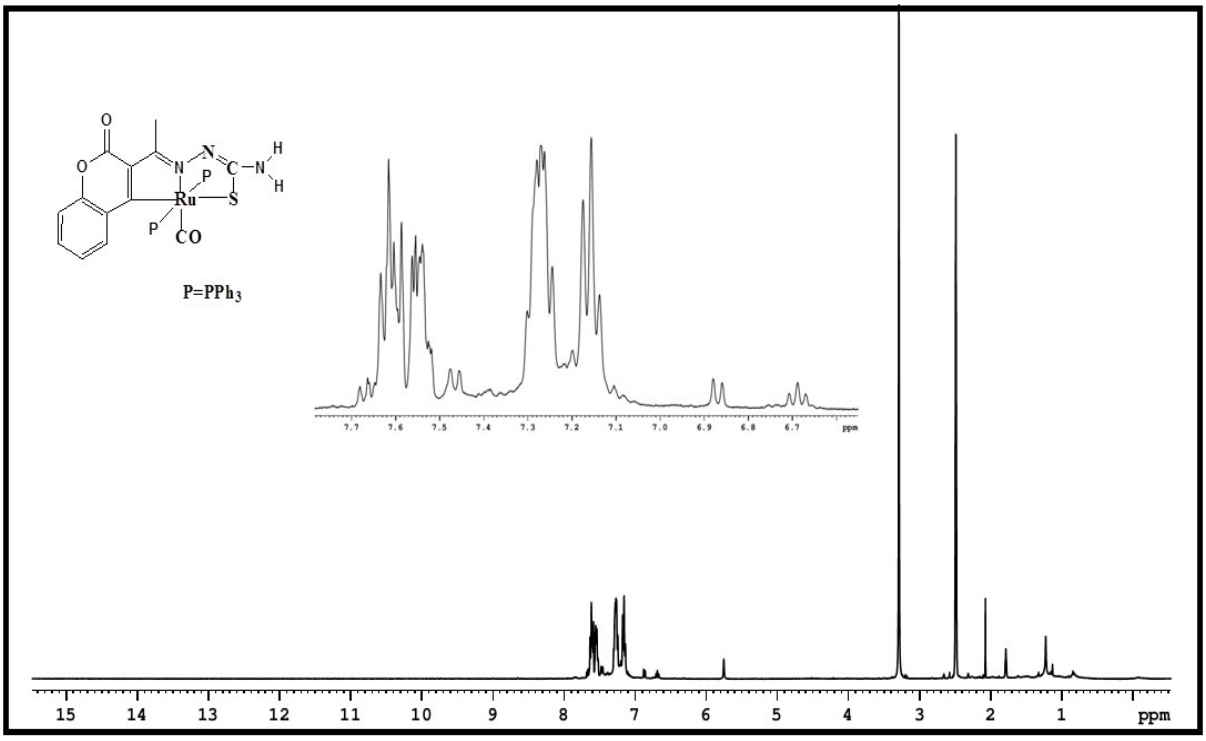

Fig. S6 ^{1}H-NMR spectrum of **[Ru(3AC-tsc)(CO)(PPh_3)$_2$] (1)**

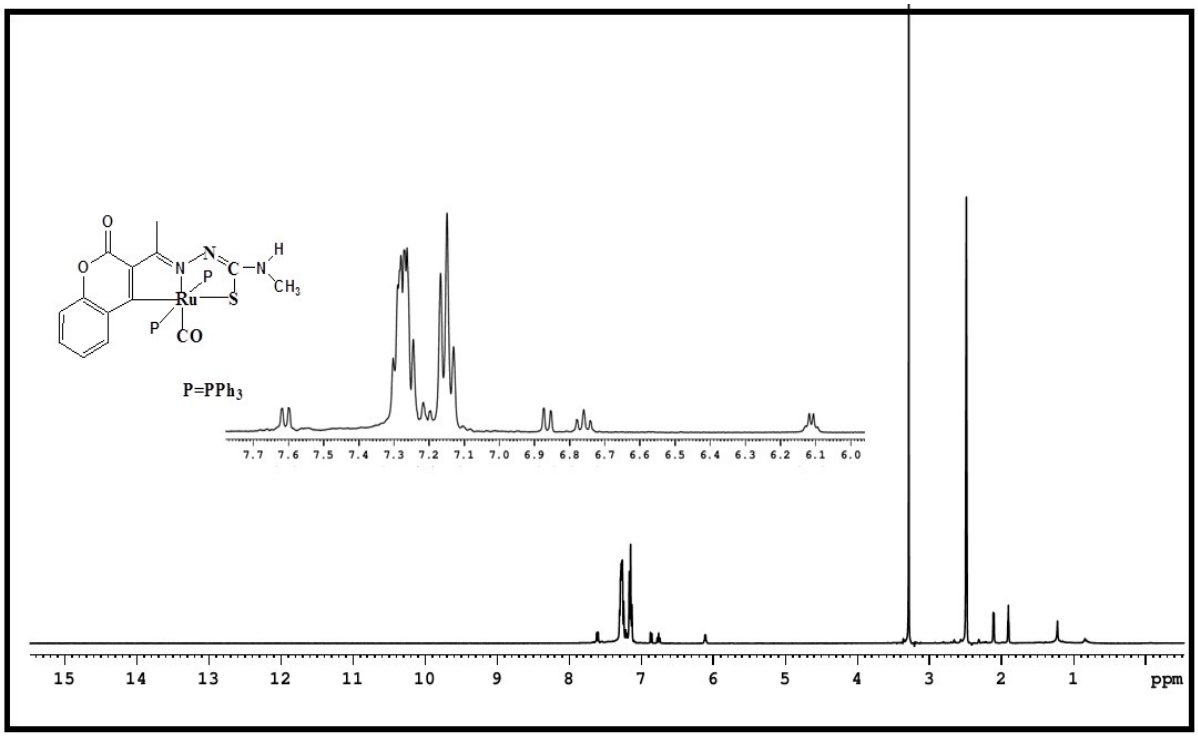

Fig. S7 ^{1}H-NMR spectrum of **[Ru(3AC-mtsc)(CO)(PPh_3)$_2$] (2)**

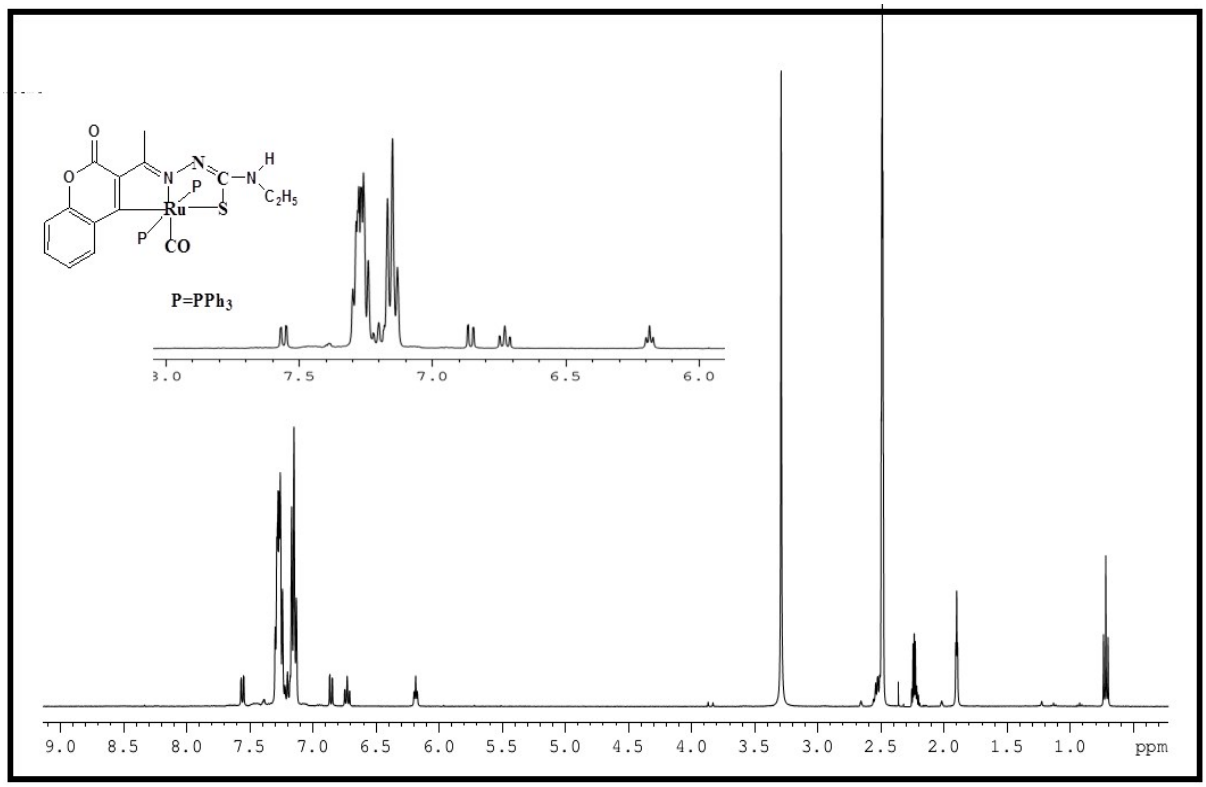

Fig. S8 ^{1}H-NMR spectrum of **[Ru(3AC-etsc)(CO)(PPh$_3$)$_2$] (3)**

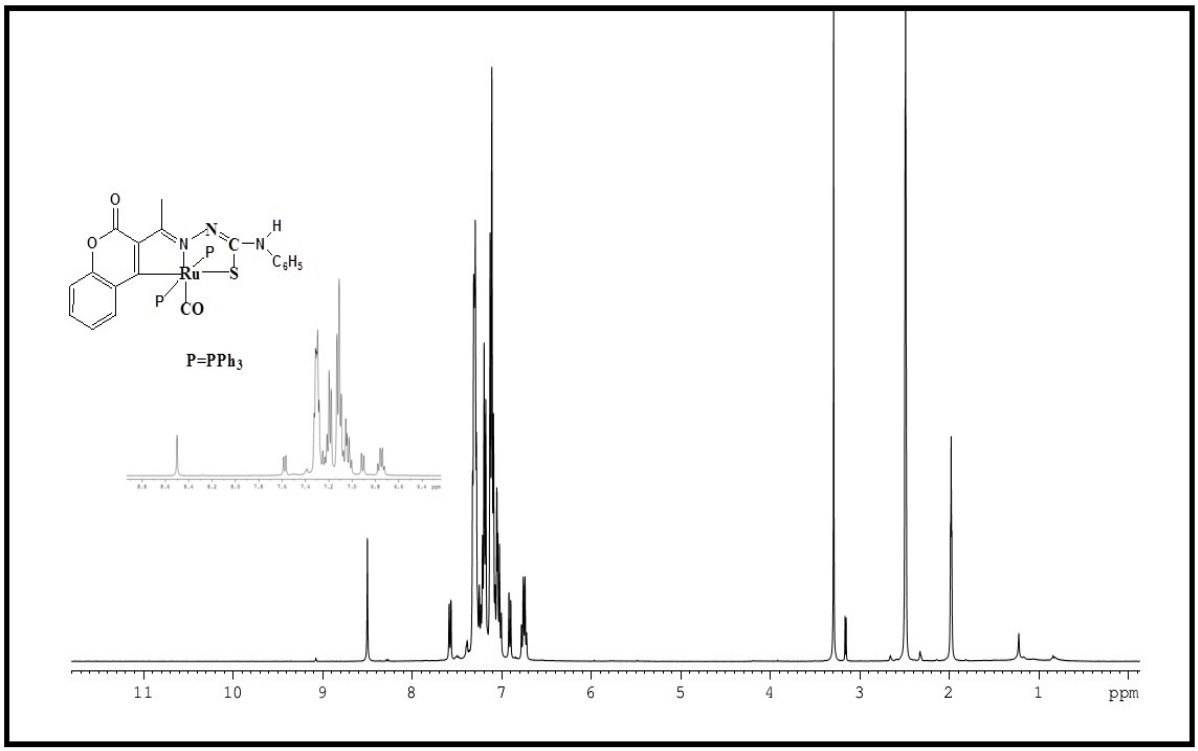

Fig. S9 ^{1}H-NMR spectrum of **[Ru(3AC-ptsc)(CO)(PPh$_3$)$_2$] (4)**

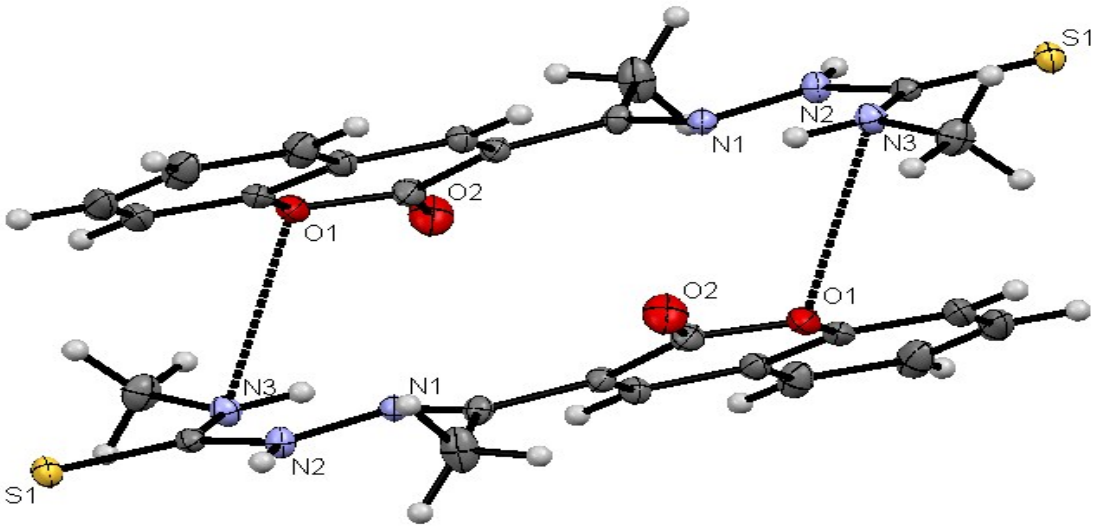

Fig. S10 ORTEP diagram of the ligand **[H_2-3AC-mtsc] (H_2L^2)** with hydrogen bonding

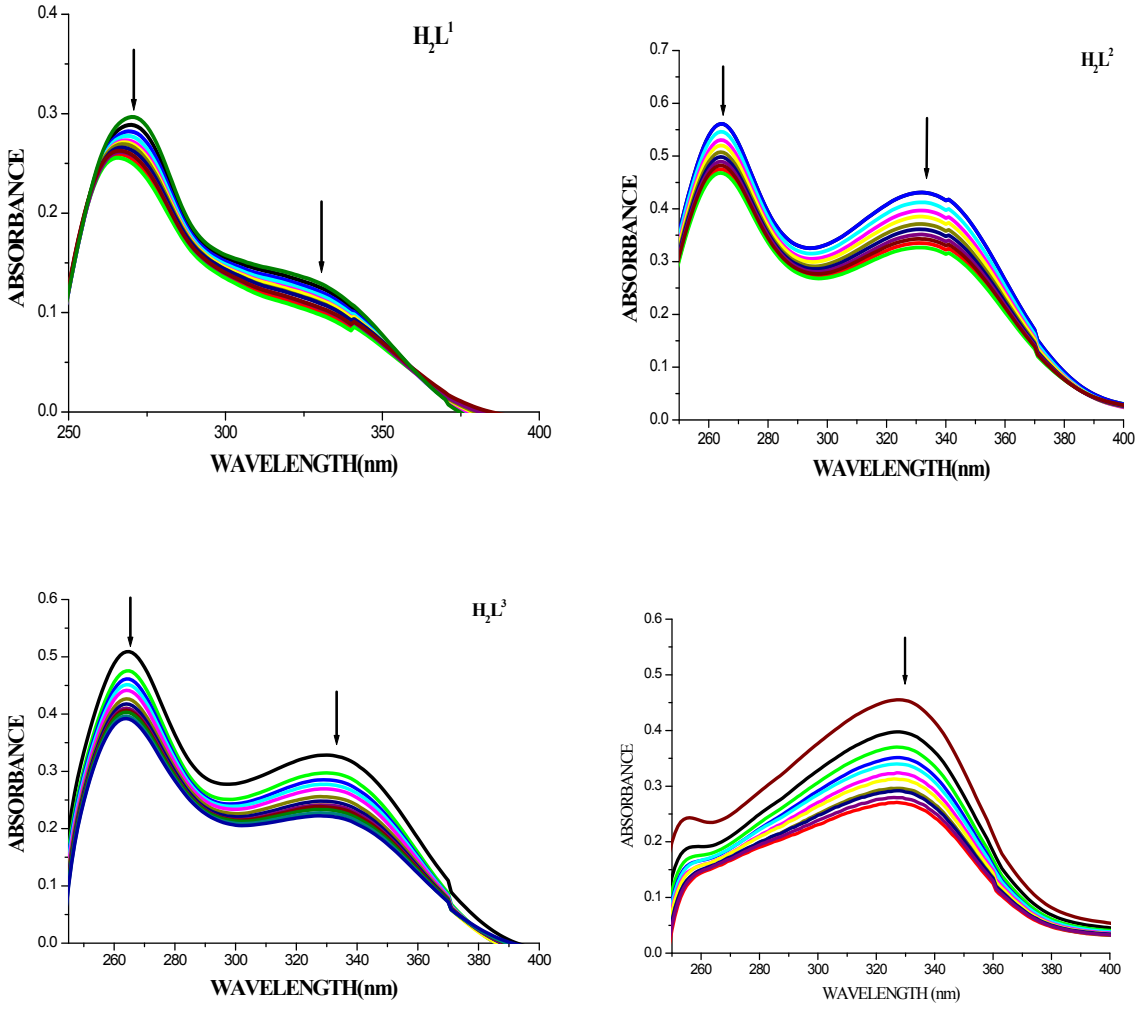

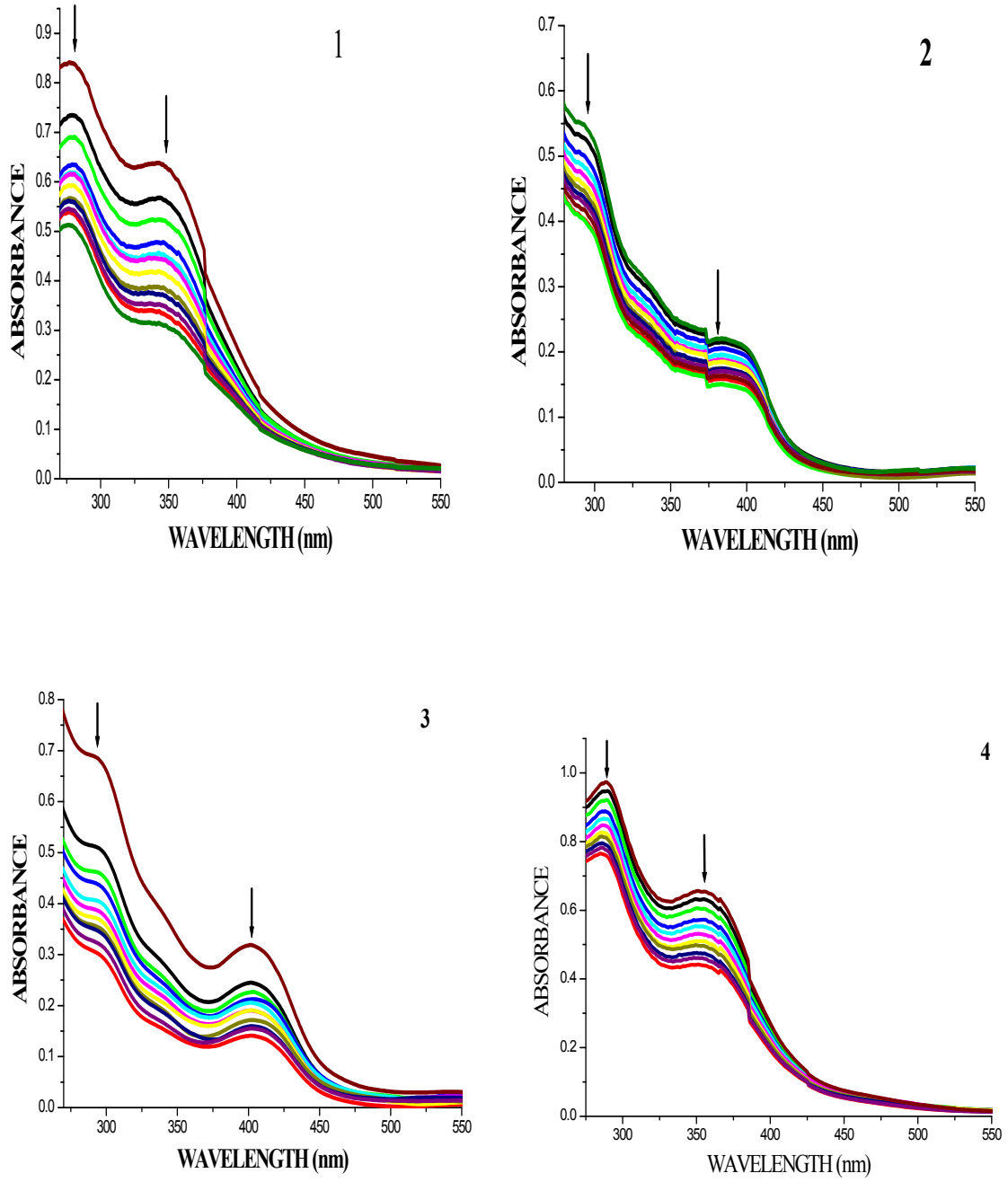

Fig. S11 Absorption titration spectra of ligands (H_2L^{1-4}) and complexes (**1-4**) (25 μM) with increasing concentrations (2.5-25μM) of CT-DNA (tris HCl buffer, pH 7.2).

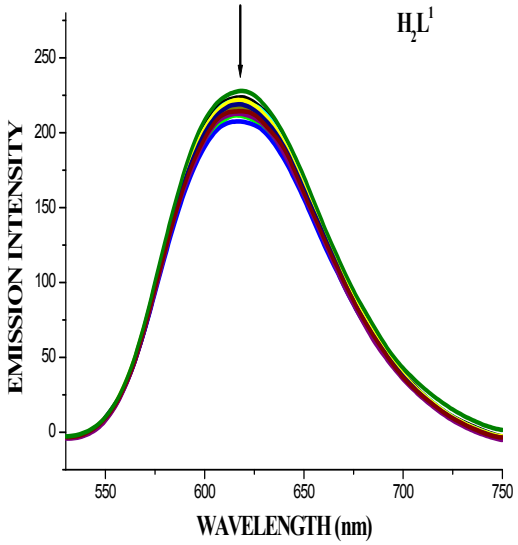
H_2L^1
EMISSION INTENSITY
WAVELENGTH (nm)
0
50
100
150
200
250
550
600
650
700
750

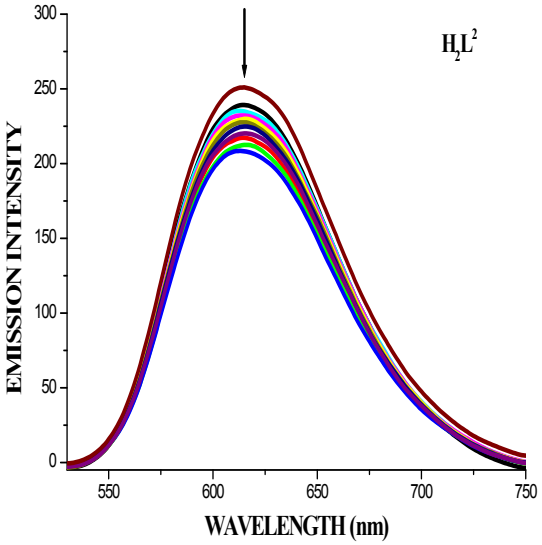
H_2L^2
EMISSION INTENSITY
WAVELENGTH (nm)
0
50
100
150
200
250
300
550
600
650
700
750

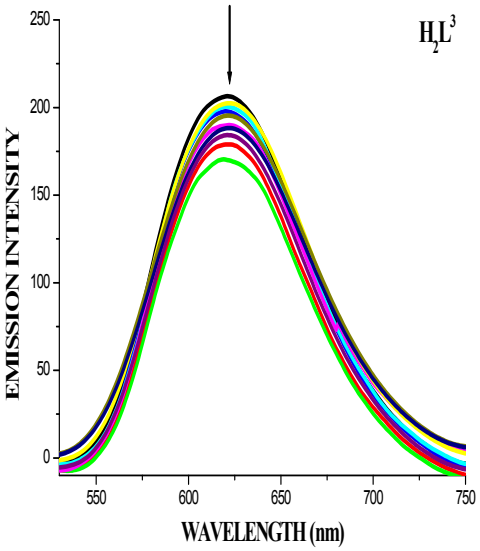
H_2L^3
EMISSION INTENSITY
WAVELENGTH (nm)
0
50
100
150
200
250
550
600
650
700
750

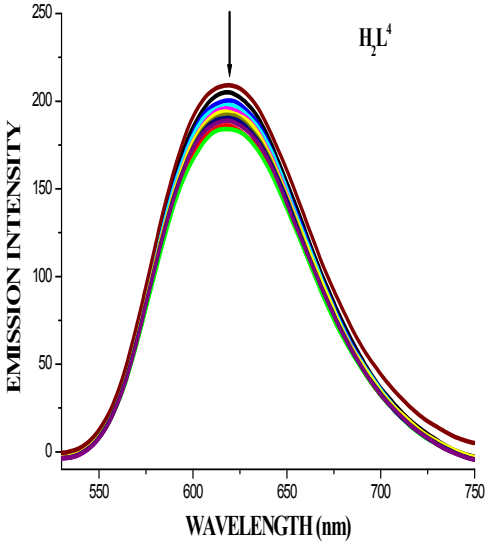
H_2L^4
EMISSION INTENSITY
WAVELENGTH (nm)
0
50
100
150
200
250
550
600
650
700
750

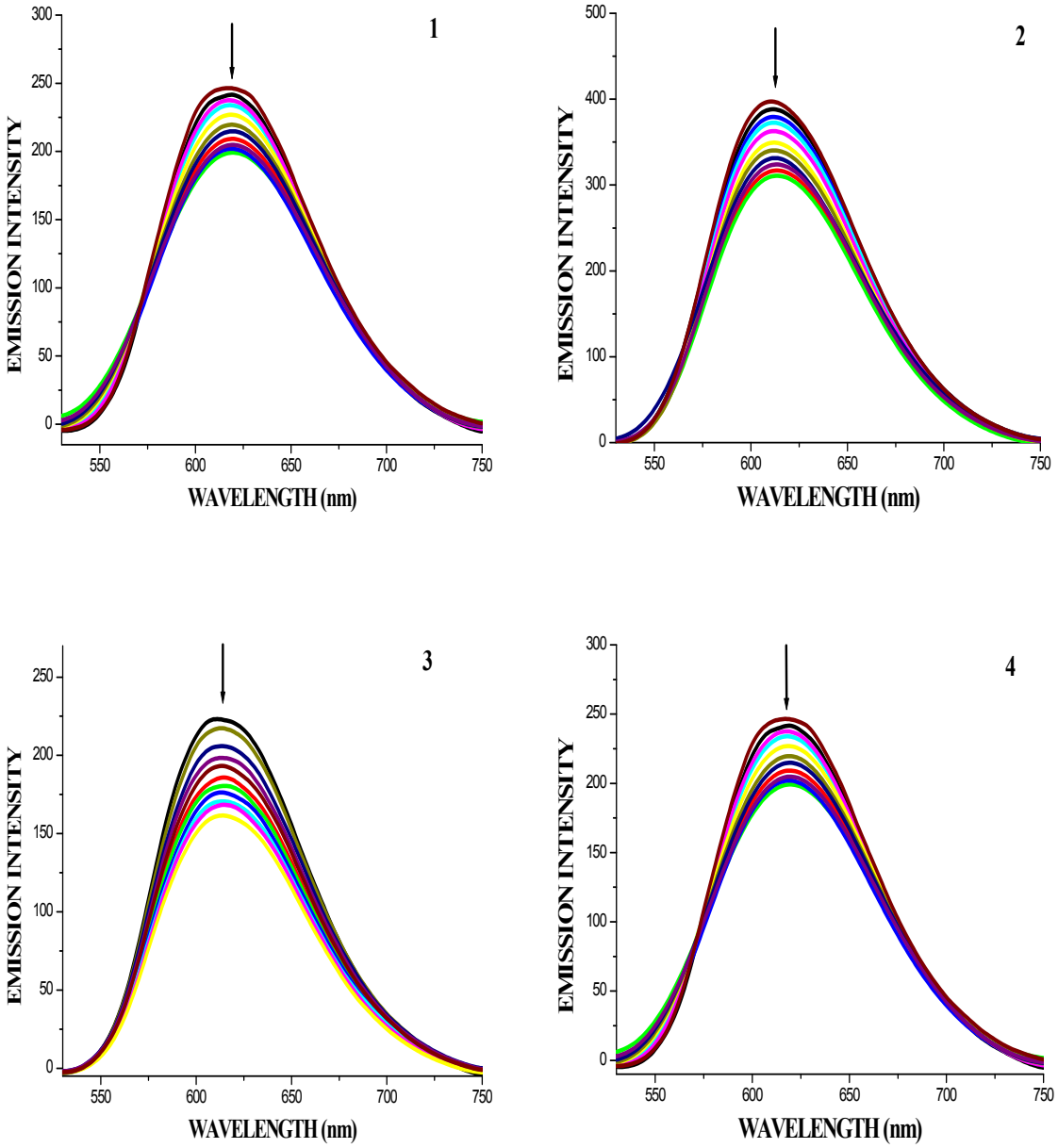

Fig. S12 The emission spectra of the DNA–EB system (λ_{exc}= 515 nm, λ_{em}= 530–750 nm), in the presence of ligands **H_2L^{1-4}** and complexs **1-4**. [DNA] = 10 μM, [Ligand] = 10–100 μM, [complex] = 10–100 μM, [EB] = 10 μM. The arrow shows the emission intensity changes upon increasing complex concentration

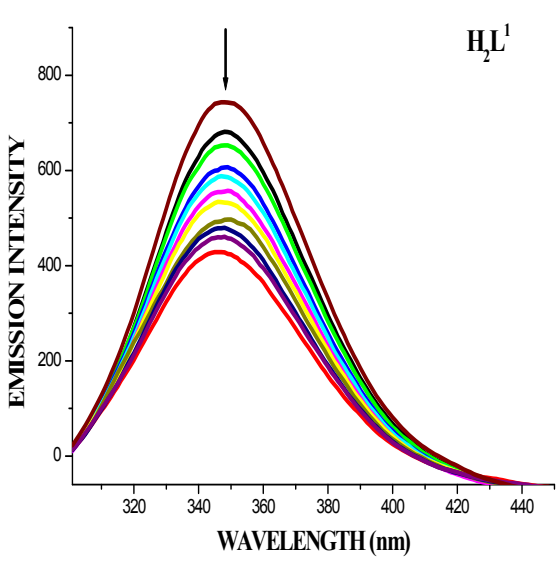
H_2L^1
EMISSION INTENSITY
WAVELENGTH (nm)

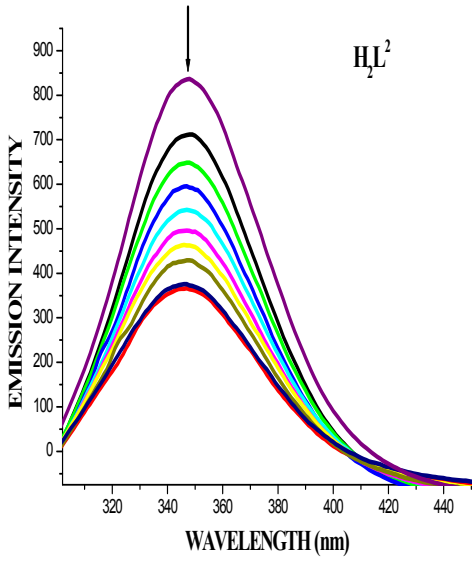
H_2L^2
EMISSION INTENSITY
WAVELENGTH (nm)

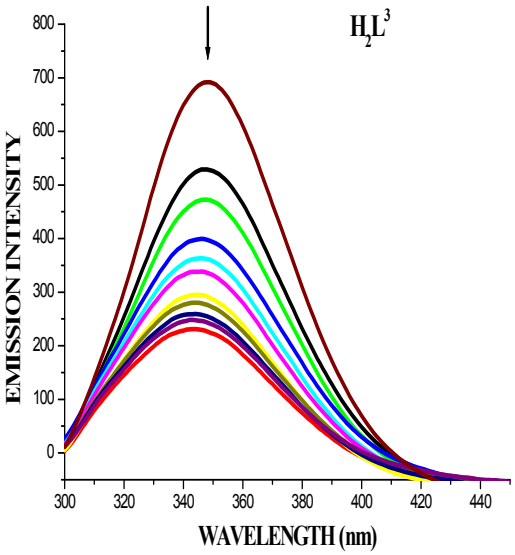
H_2L^3
EMISSION INTENSITY
WAVELENGTH (nm)

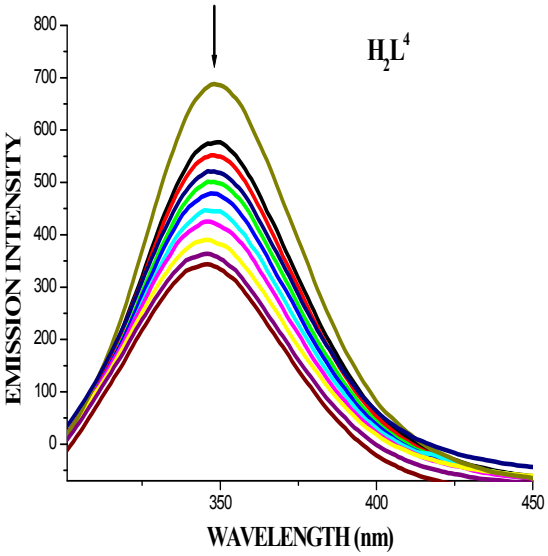
H_2L^4
EMISSION INTENSITY
WAVELENGTH (nm)

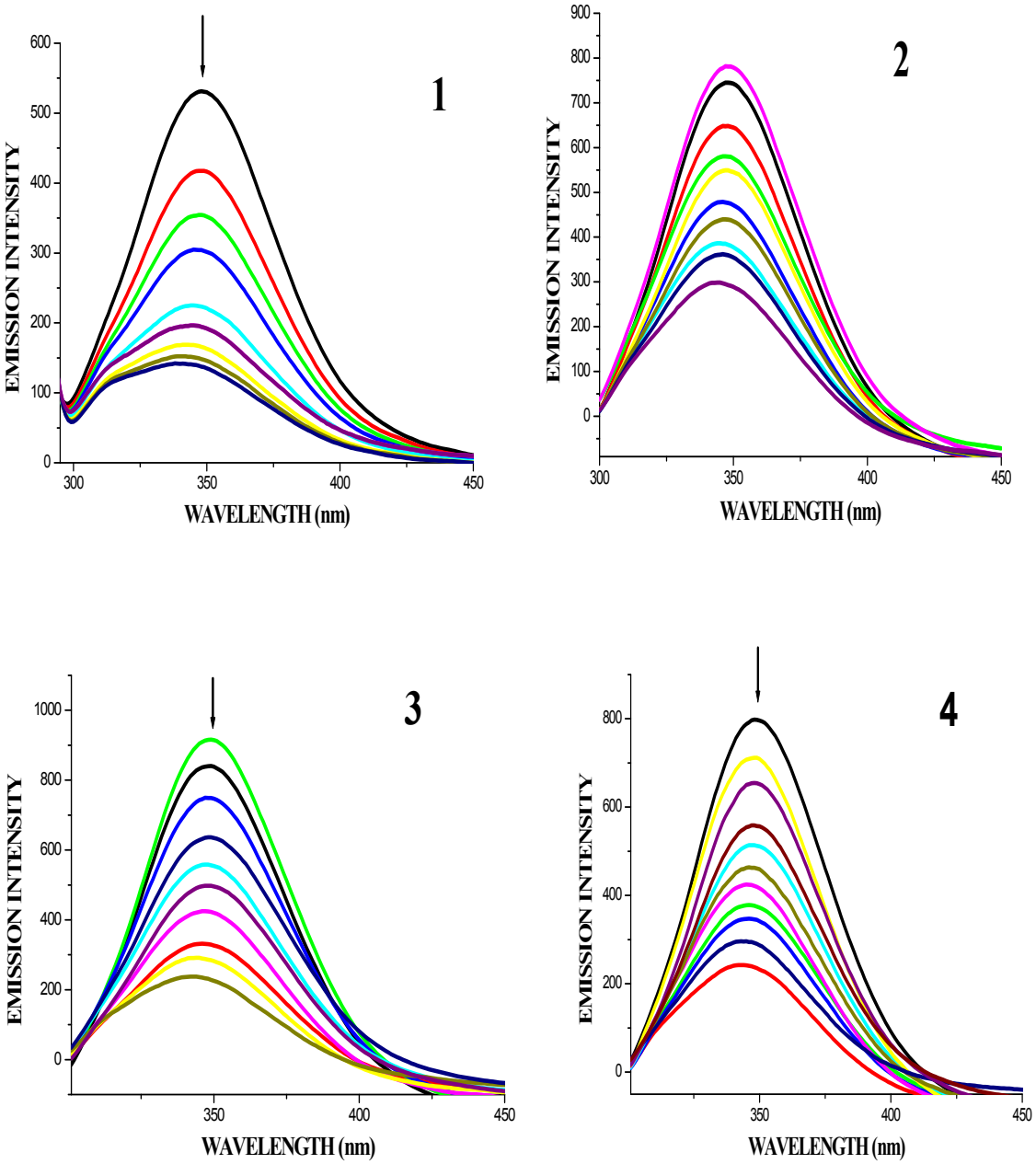

Fig. S13 The emission spectra of BSA (10 μM; λexc= 280 nm; λemi= 346 nm) in the presence of increasing amounts of ligands $\mathbf{H_2L^{1\text{-}4}}$ and complexes **1-4** (10–100 μM). The arrow shows the emission intensity changes upon increasing complex concentration

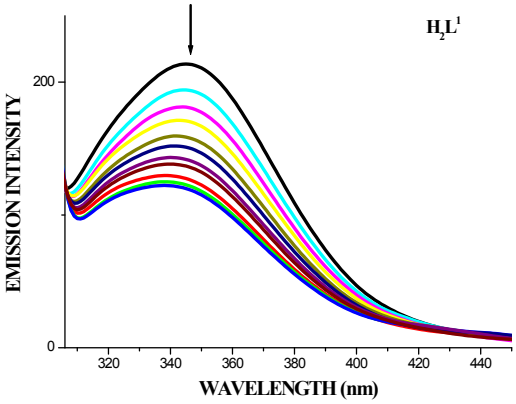
H_2L^1
EMISSION INTENSITY
WAVELENGTH (nm)

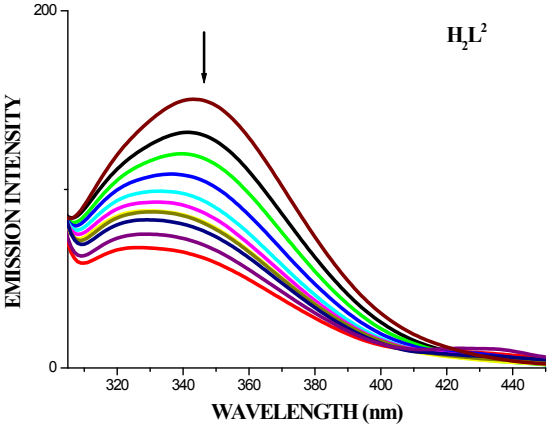
H_2L^2
EMISSION INTENSITY
WAVELENGTH (nm)

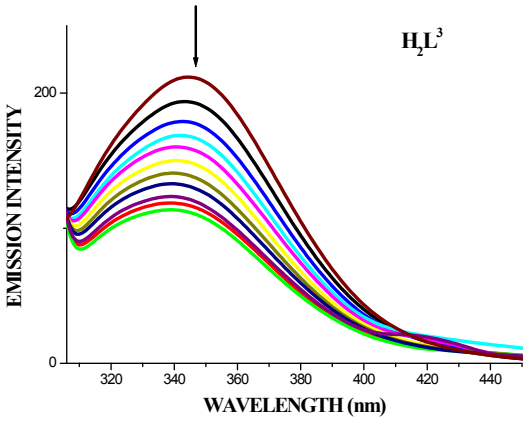
H_2L^3
EMISSION INTENSITY
WAVELENGTH (nm)

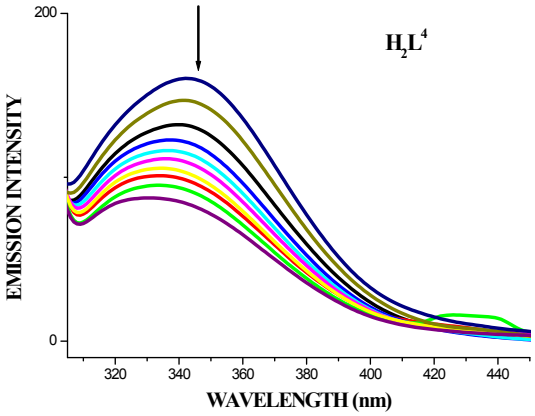
H_2L^4
EMISSION INTENSITY
WAVELENGTH (nm)

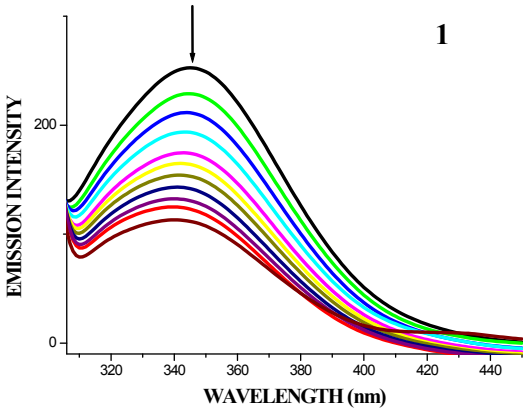
1
EMISSION INTENSITY
WAVELENGTH (nm)

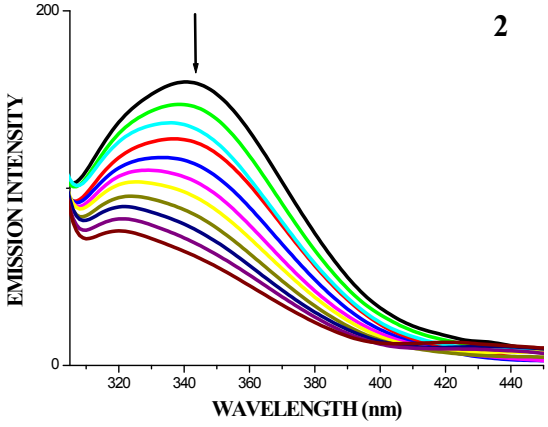
2
EMISSION INTENSITY
WAVELENGTH (nm)

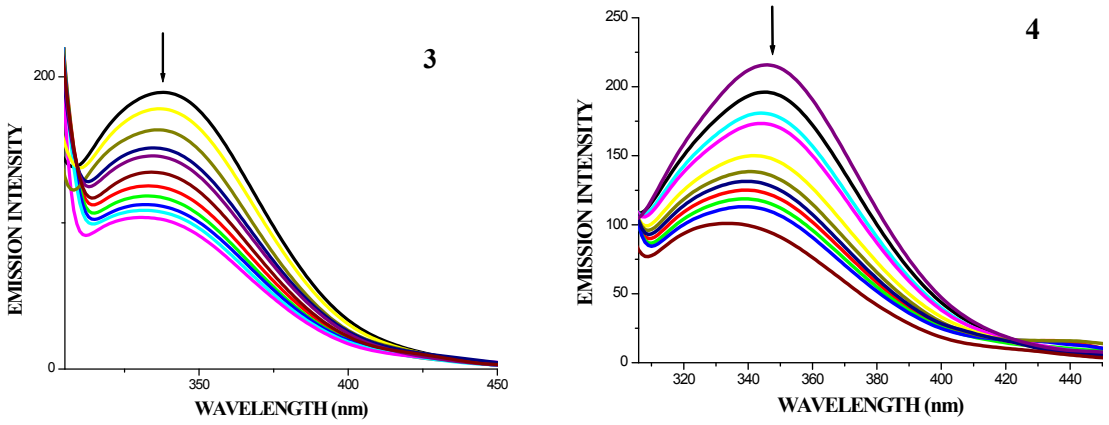

Fig. S14 The emission spectra of HSA (10 μM; λexc= 290 nm; λemi= 345 nm) in the presence of increasing amounts of ligands $\mathbf{H_2L^{1\text{-}4}}$ and complexes **1-4** (10–100 μM). The arrow shows the emission intensity changes upon increasing complex concentration

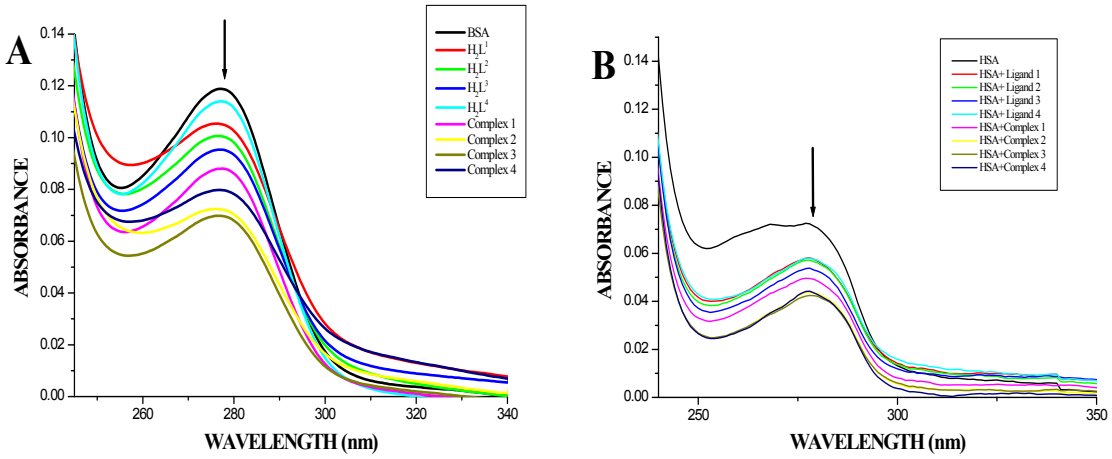

Fig. S15 A) Absorption spectra of absence and presence of ligands $\mathbf{H_2L^{1\text{-}4}}$ and complexes (**1-4**) with BSA (1×10^{-5}M) **B)** Absorption spectra of absence and presence of ligands $\mathbf{H_2L^{1\text{-}4}}$ and complexes (**1-4**) with HSA (1×10^{-5}M)

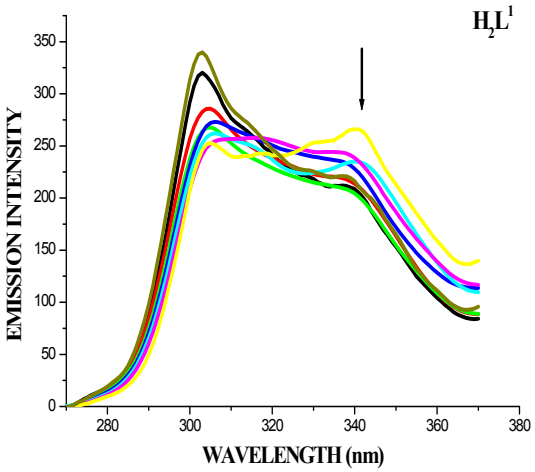
H_2L^1
EMISSION INTENSITY
WAVELENGTH (nm)

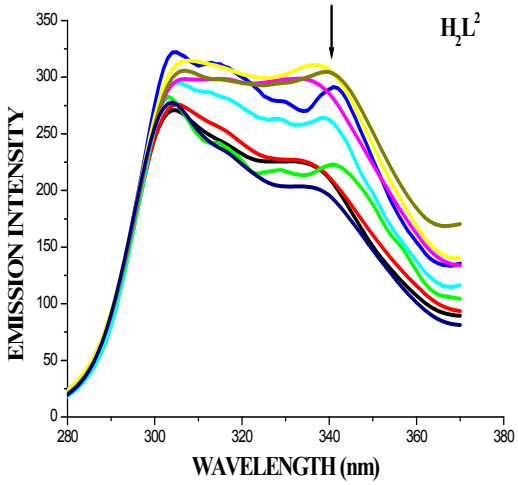
H_2L^2
EMISSION INTENSITY
WAVELENGTH (nm)

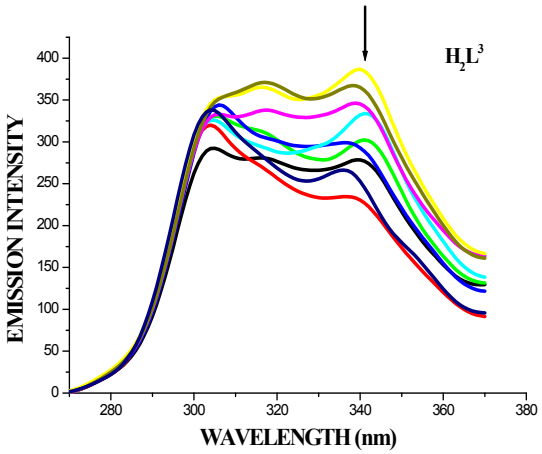
H_2L^3
EMISSION INTENSITY
WAVELENGTH (nm)

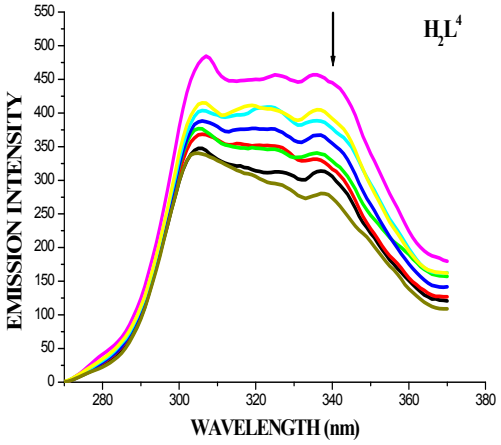
H_2L^4
EMISSION INTENSITY
WAVELENGTH (nm)

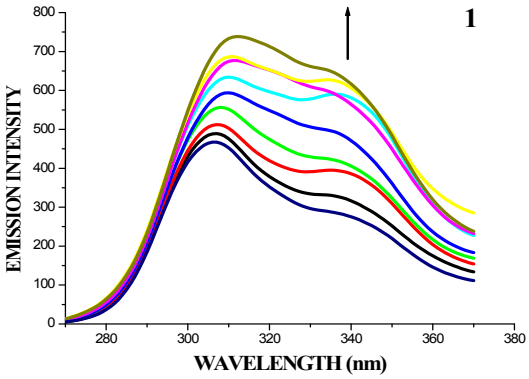
1
EMISSION INTENSITY
WAVELENGTH (nm)

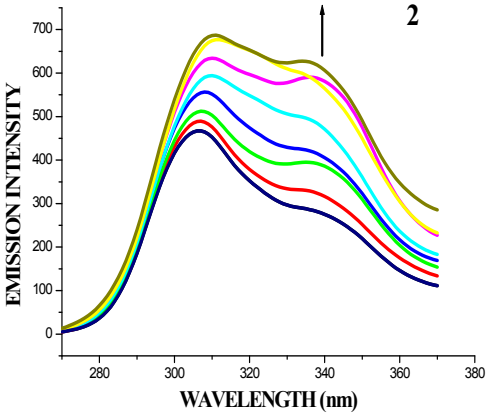
2
EMISSION INTENSITY
WAVELENGTH (nm)

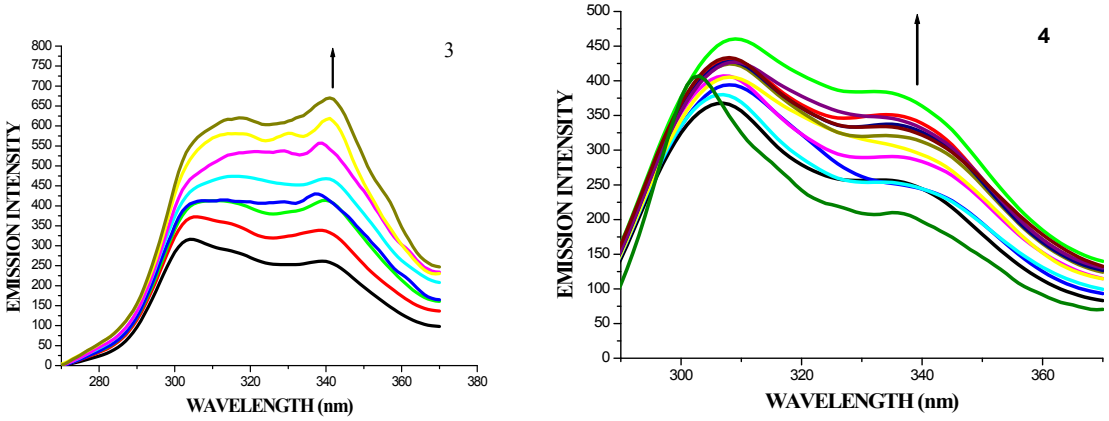

Fig. S16 Synchronous spectra of BSA (10 μM) in the presence of increasing amounts of ligands $\mathbf{H_2L^{1\text{-}4}}$ and complexes **1-4** (10–100 μM) for a wavelength difference of Δλ= 15 nm. The arrow shows the emission intensity changes upon increasing concentration of compounds

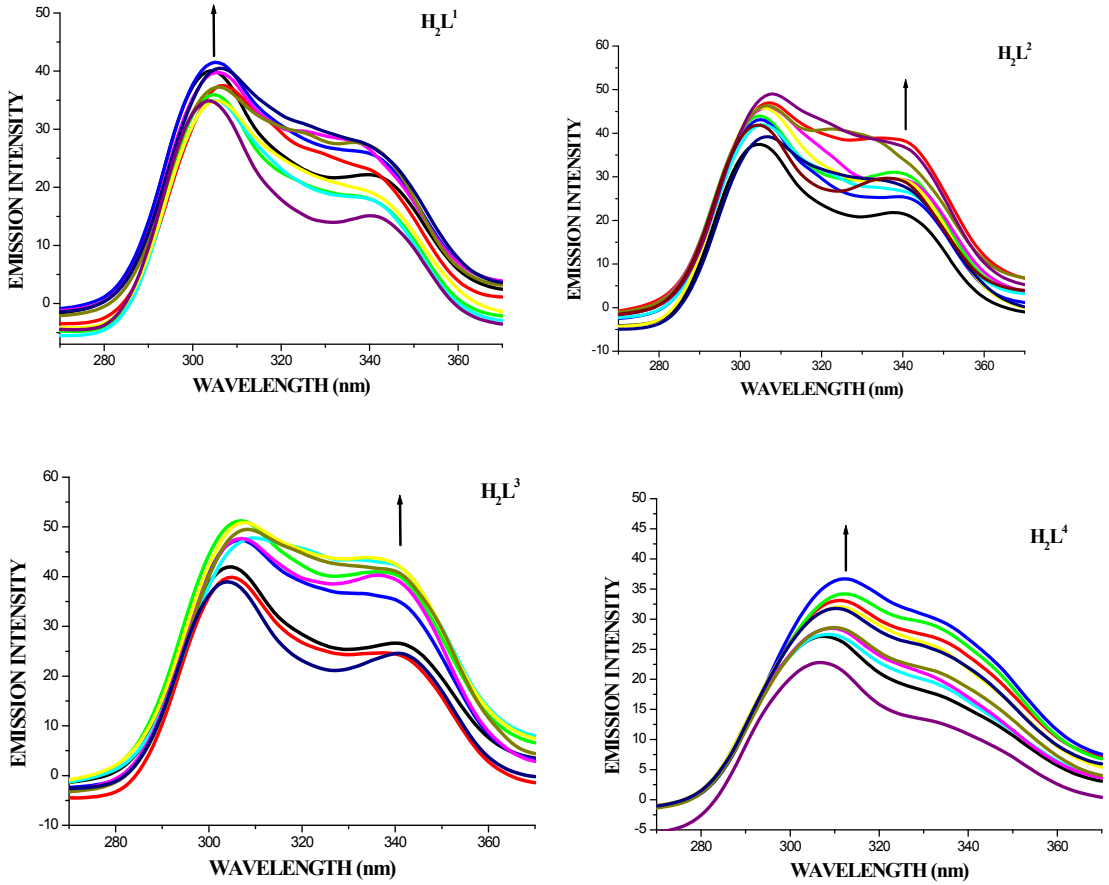

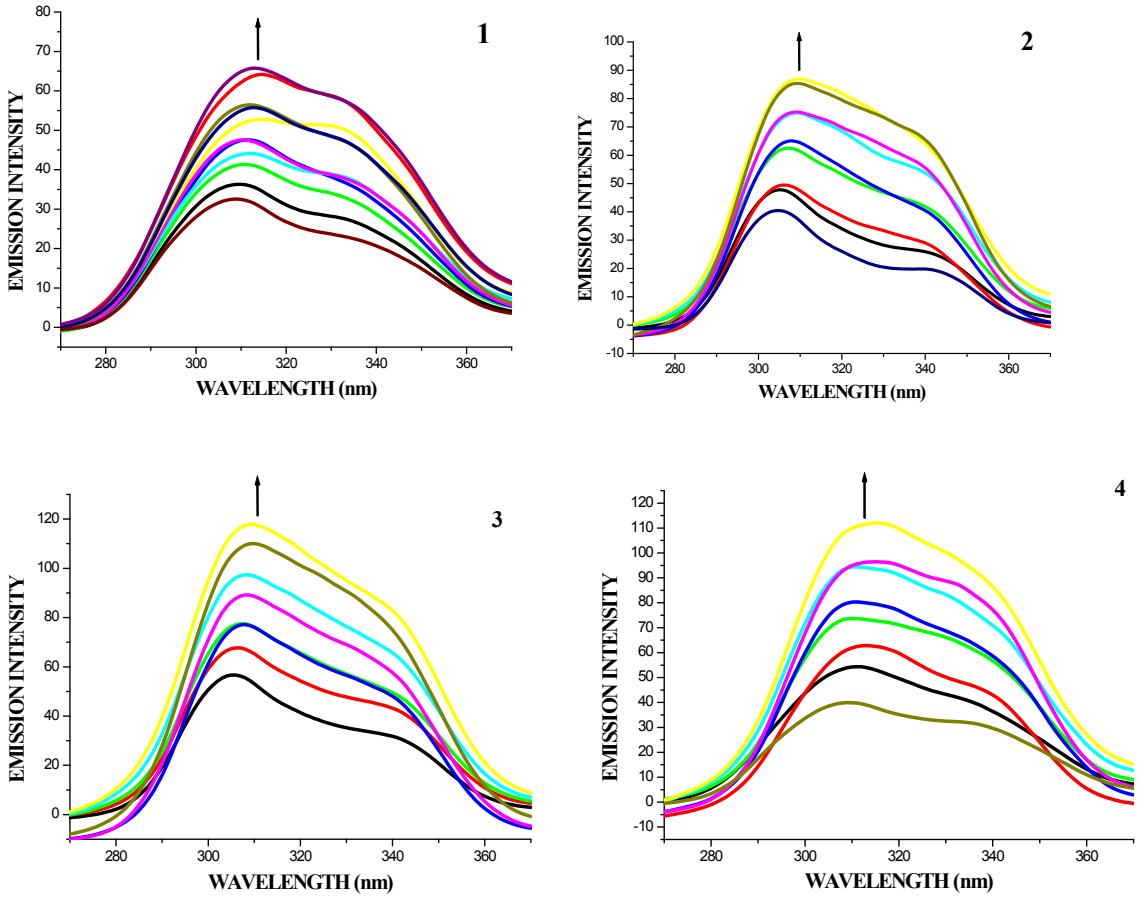

Fig. S17 Synchronous spectra of HSA (10 μM) in the presence of increasing amounts of ligands $\mathbf{H_2L^{1\text{-}4}}$ and complexes **1-4** (10–100 μM) for a wavelength difference of Δλ= 15 nm. The arrow shows the emission intensity changes upon increasing concentration of compounds

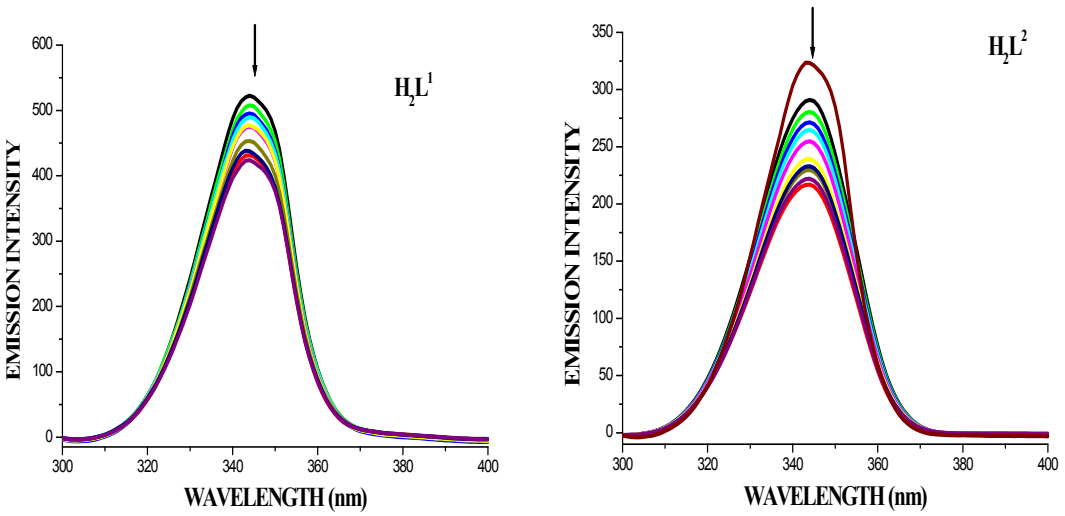

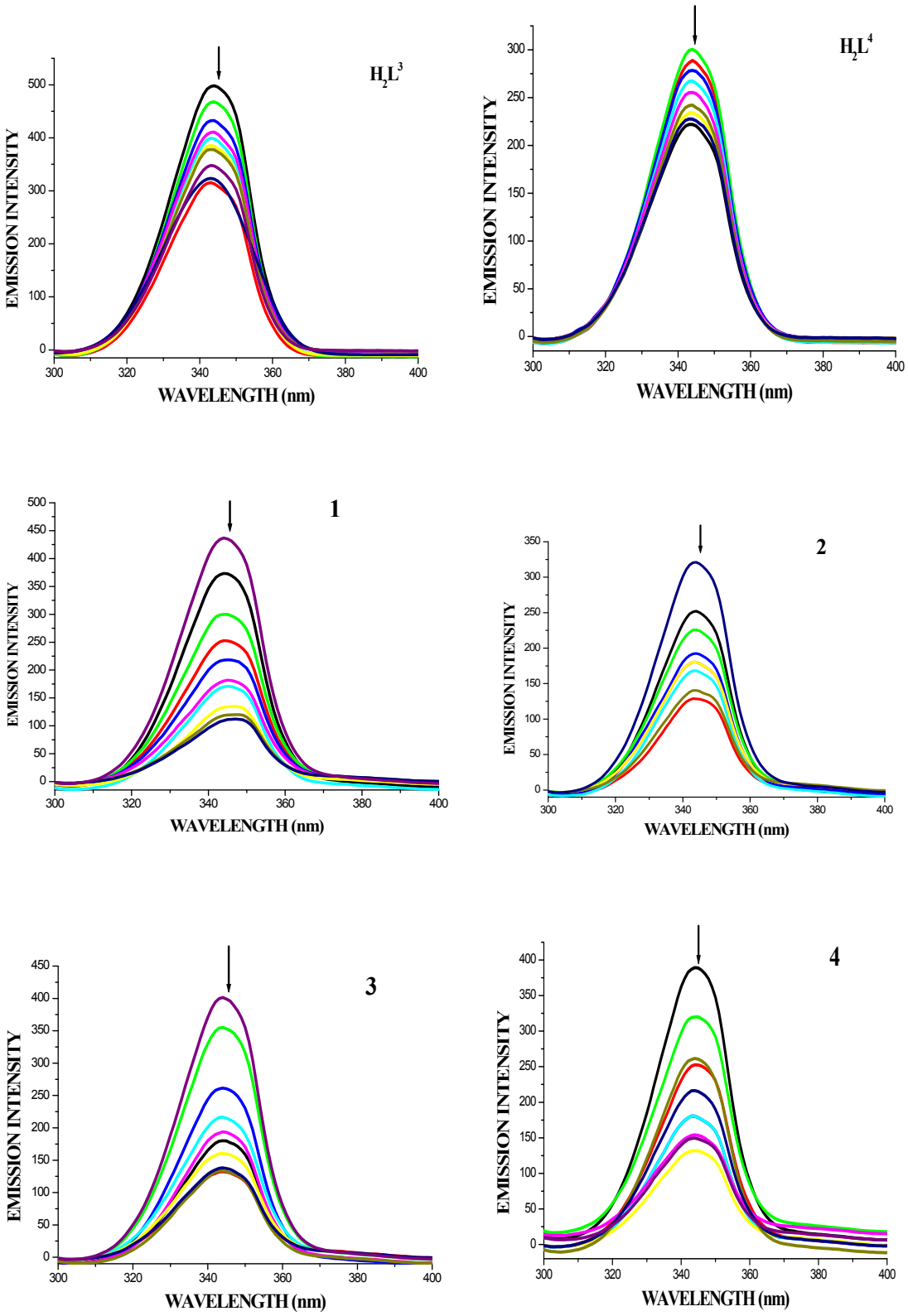

Fig. S18 Synchronous spectra of BSA (10 μM) in the presence of increasing amounts of ligands $\mathbf{H_2L^{1\text{-}4}}$ and complexes **1-4** (10–100 μM) for a wavelength difference of Δλ= 60 nm. The arrow shows the emission intensity changes upon increasing concentration of compounds

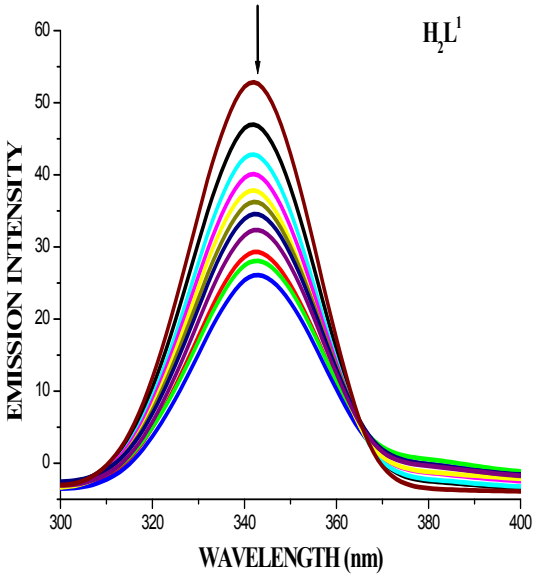
H_2L^1
EMISSION INTENSITY
WAVELENGTH (nm)

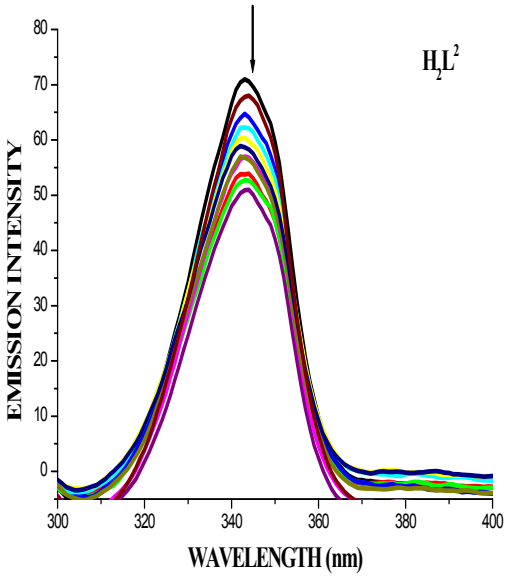
H_2L^2
EMISSION INTENSITY
WAVELENGTH (nm)

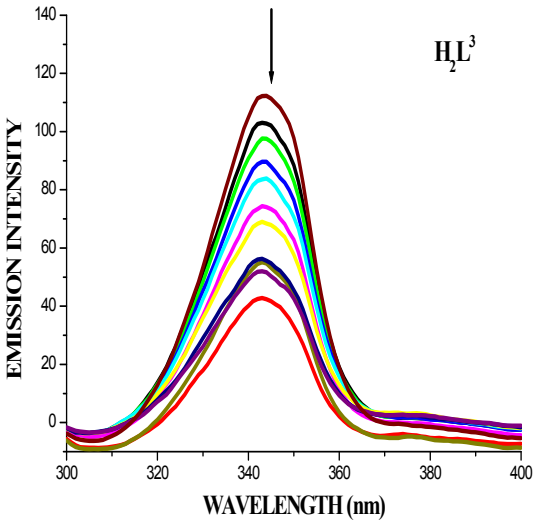
H_2L^3
EMISSION INTENSITY
WAVELENGTH (nm)

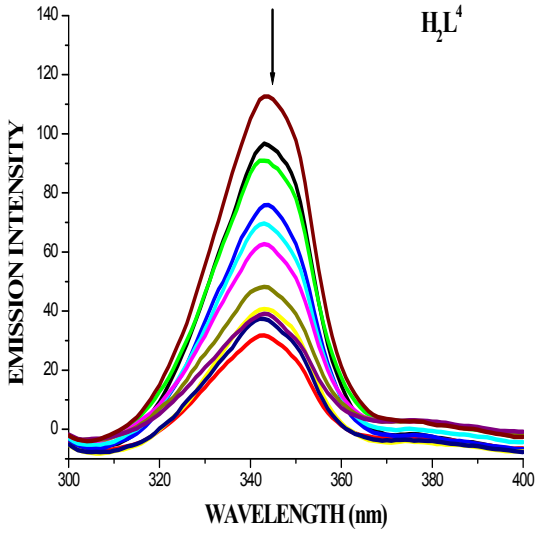
H_2L^4
EMISSION INTENSITY
WAVELENGTH (nm)

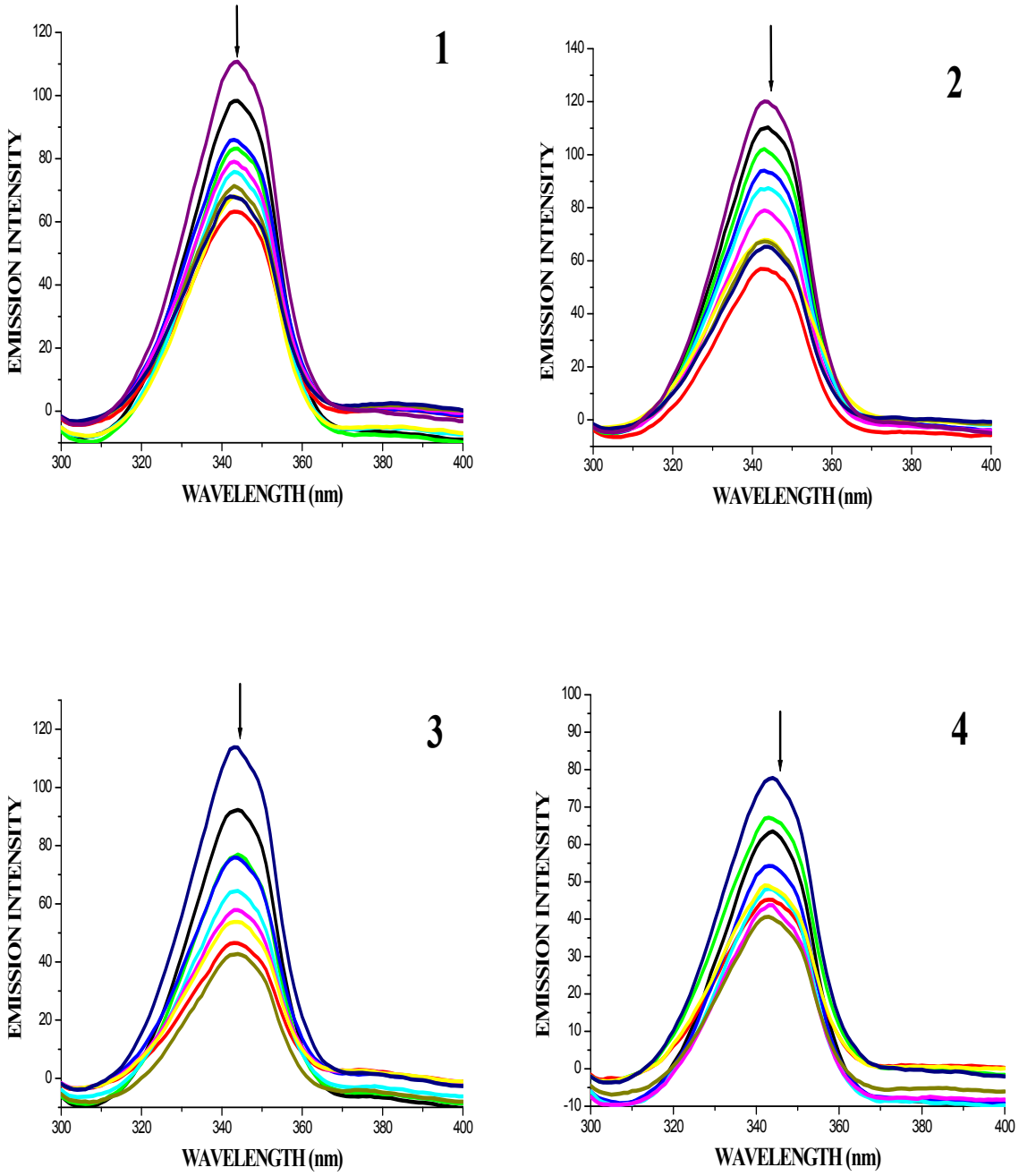

Fig. S19 Synchronous spectra of HSA (10 μM) in the presence of increasing amounts of ligands $\mathbf{H_2L^{1\text{-}4}}$ and complexes **1-4** (10–100 μM) for a wavelength difference of Δλ= 60 nm. The arrow shows the emission intensity changes upon increasing concentration of compounds